Molecular and Epigenetic Consequences of Short-Term Hypoxia Exposure in Rainbow Trout (*Oncorhynchus mykiss*)

William Johnston

Thesis submitted to the University of Ottawa in partial fulfillment of the requirements for the Master of Science in Biology

Department of Biology
Faculty of Science
University of Ottawa

ACKNOWLEDGEMENTS

I would not have been able to complete my Master's thesis without the help of many wonderful people. First of all, I would like to thank my supervisor, Jan Mennigen, for his exceptional support and guidance throughout my project. You were always there to answer my questions and keep me going when I questioned my own abilities. I would also like to thank my Thesis Advisor Committee members Katie Gilmour and Bill Willmore. You gave wonderful and valuable feedback and support for this project. I would also like to thank Jean-Michel Weber, who while retired still provided excellent feedback. I would like to thank the members of the Mennigen Lab, past and present, who trained, helped, and supported me throughout this project; Giancarlo Talarico, Sally Adil, Niepukolie Nipu, Dinusha Rajapaksha, Catherine Cao, Lai Wei, and Hyojin Lee. I would also like to thank Kaitlyn Flear from the Gilmour lab for all her help with the exposure setup as well as Gilda Stefanelli, Karanveer Johal, and the rest of the Stefanelli lab for their help with the ChIP assays. Finally, I would like to thank Nicole Nagy for your help with the qPCR use in the Common Core lab.

ABSTRACT

Environmental hypoxia affects freshwater systems, and acute hypoxic events are expected to increase in frequency with climate change. Rainbow trout (*Oncorhynchus mykiss*), a salmonid species of economic and cultural importance in Canada and introduced to freshwaters across most continents, is an active species that is sensitive to environmental hypoxia. In this thesis, I investigate the hypothesis that rainbow trout acutely exposed to mild (50% oxygen saturation) and severe (25% oxygen saturation) hypoxia exhibit rapid metabolic changes which are indicative of anerobic glycolytic and are, at least in part, mediated at the gene expression level and I hypothesize that these changes in gene expression are mediated by histone modifications. While glucose and lipid metabolite concentrations are not significantly affected by acute hypoxia exposure suggesting tight regulation to maintain steady-state, transcripts coding for key components of glucose, lactate, and lipid transcripts are differentially induced in a tissue-specific manner. Hepatic transcripts were most sensitive to hypoxia, favouring induction of transcripts related to glucose metabolism like in white muscle tissue. Under severe hypoxia exposure, coordinated expression of transcripts related to lipid metabolism was observed in liver, but also muscle and adipose tissue, possibly indicating a scavenging response of peroxided lipids rather than a use as fuel. When probing a role for the O_2-sensitive epigenetic mark H3K4me3 in upstream prompter regions of induced hepatic genes *mct1* and *pck1*, no clear relationship between O_2-dependent regulation of this mark and gene expression was found, suggesting other transcriptional control mechanisms are involved. Together, this thesis provides novel insight into molecular underpinnings and thresholds of tissue-specific metabolic responses in rainbow trout and opens the field for future comparative investigation of epigenetic mechanisms of responses to hypoxia in fishes.

RÉSUMÉ

L'hypoxie environnementale affecte les systèmes d'eau douce et les événements hypoxiques aigus devraient augmenter en fréquence avec le changement climatique. La truite arc-en-ciel (*Oncorhynchus mykiss*), une espèce de salmonidé d'importance économique et culturelle au Canada et introduite dans les eaux douces de la plupart des continents, est une espèce active qui est sensible à l'hypoxie environnementale. Dans cette thèse, j'étudie l'hypothèse selon laquelle la truite arc-en-ciel est exposée de manière aiguë à une hypoxie légère (50% de saturation en oxygène) et sévère (25% de saturation en oxygène) présente des changements métaboliques rapides qui sont indicatifs d'une glycolyse anaérobie et qui sont, au moins en partie, médiés au niveau de l'expression des gènes et j'émets l'hypothèse que ces changements dans l'expression des gènes sont médiés par des modifications d'histones. Alors que les concentrations de métabolites de glucose et de lipides ne sont pas significativement affectées par une exposition aiguë à l'hypoxie, ce qui suggère une régulation étroite pour maintenir l'état d'équilibre, les transcrits codant pour les composants clés du métabolisme du glucose, du lactate et des lipides sont induits de manière différentielle et spécifique à chaque tissu. Les transcrits hépatiques étaient les plus sensibles à l'hypoxie, favorisant l'induction de transcrits liés au métabolisme du glucose similaires à ceux du tissu musculaire blanc. Lors d'une exposition à l'hypoxie plus sévère, une expression coordonnée des transcrits liés au métabolisme des lipides a été observée dans le foie, mais aussi dans le muscle et le tissu adipeux, ce qui pourrait indiquer une réponse de piégeage des lipides peroxydés plutôt qu'une utilisation comme carburant. Lors de l'étude du rôle de la marque épigénétique H3K4me3 sensible à l'O_2 dans les régions prompteurs en amont des gènes hépatiques induits *mct1* et *pck1*, aucune relation claire entre la régulation dépendante de l'O_2 de cette marque et l'expression génique n'a été trouvée, ce qui suggère que d'autres mécanismes de contrôle

transcriptionnel sont impliqués. Cette thèse apporte un éclairage nouveau sur les fondements moléculaires et les seuils des réponses métaboliques spécifiques aux tissus chez la truite arc-en-ciel, et ouvre la voie à de futures études comparatives des mécanismes épigénétiques des réponses à l'hypoxie chez les poissons.

TABLE OF CONTENTS

LIST OF FIGURES AND TABLES

LIST OF ABBREVIATIONS

5-hmc	5-hydroxymethylcytosine
5-mC	5-methylcytosine
Acyl-CoA	Acyl coenzyme A
ADP	Adenosine diphosphate
ANOVA	Analysis of variance
ASR	Aquatic surface respiration
ATP	Adenosine triphosphate
bp	Base pair
Cd36	Fatty acid translocase protein (cluster of differentiation 36)
cd36	Fatty acid translocase gene
cDNA	Complementary deoxyribonucleic acid
ChIP	Chromatin immunoprecipitation
Cpt1a	Carnine palmitoyltransferase protein
cpt1a	Carnine palmitoyltransferase gene
CT	Cycle threshold
DEPC	Diethyl pyrocarbonate
DNA	Deoxyribonucleic acid
DO	Dissolved oxygen
ef1a	Elongation factor 1A gene
EGLN	Egl-9 family hypoxia inducible factor protein
egln1	Egl-9 family hypoxia inducible factor 1 gene
egln2	Egl-9 family hypoxia inducible factor 2 gene
egln3	Egl-9 family hypoxia inducible factor 3 gene
EtOH	Ethanol
Fasn	Fatty acid synthase protein
fasn	Fatty acid synthase gene
F-Primer	Forward primer
G	1 Earth gravity (9.8 m/s^2)
Gck	Glucokinase protein
gcka	Glucokinase a gene
gDNA	Genomic deoxyribonucleic acid
g	Gram
Glut4	Glucose transporter type 4 protein
glut4b	Glucose transporter type 4b gene
GSI	Gonadosomatic index
H3	Unmethylated histone H3
H3K4	Lysine 4 of histone H3
H3K4me3	Histone H3 trimethylated at lysine 4
H3K27me3	Histone H3 trimethylated at lysine 27
HIF-1α	Hypoxia-inducible factor 1α
HIF-1β	Hypoxia-inducible factor 1β
Hoad	3-hydroxyacyl-CoA dehydrogenase protein
hoad	3-hydroxyacyl-CoA dehydrogenase gene
HPI	Hypothalamo-pituitary-interrenal

HRE	Hypoxia-response elements
Hsl	Hormone-sensitive lipase protein
hsl	Hormone-sensitive lipase gene
IgG	Immunoglobulin G
KDM	Lysine demethylase
KDM5A	Lysine demethylase 5A
KDM6A	Lysine demethylase 6A
Km	Michaelis constant
KMT2	Lysine methyltransferase 2
L	Litre
Ldh	Lactate dehydrogenase protein
Ldha	Lactate dehydrogenase a protein
ldha	Lactate dehydrogenase a gene
Ldhba	Lactate dehydrogenase ba protein
Ldhbb	Lactate dehydrogenase bb protein
ldhbb	Lactate dehydrogenase bb gene
Ldhd	Lactate dehydrogenase d protein
ldhd	Lactate dehydrogenase d gene
LiCl	Lithium chloride
LOE	Loss of equilibrium
Lpl	Lipoprotein lipase protein
lpl	Lipoprotein lipase gene
Mct	Monocarboxylate transporter protein
mct	Monocarboxylate transporter gene
Mct1a	Monocarboxylate transporter 1a protein
Mct1b	Monocarboxylate transporter 1b protein
mct1	Monocarboxylate transporter 1 gene
Mct2	Monocarboxylate transporter 2 protein
mct2	Monocarboxylate transporter 2 gene
Mct4	Monocarboxylate transporter 4 protein
Mdh	Malate dehydrogenase protein
mg	Milligram
µg	Microgram
µL	Microlitre
MS-222	Tricane mesylate
NaCl	Sodium chloride
NEFA	Non-esterified fatty acid
NEM	N-ethylmaleimide
nm	Nanometre
O_2	Molecular oxygen
PBS	Phosphate buffered saline
Pck1	Phosphoenolpyruvate carbokinase 1 protein
pck1	Phosphoenolpyruvate carbokinase 1 gene
PCR	Polymerase chain reaction
Pepck	Phosphoenolpyruvate carbokinase protein
Phd	2-oxyglutatare-dependent prolyl hydroxylase protein

Phd3	2-oxyglutatare-dependent prolyl hydroxylase 3 protein
pO_2	Partial pressure of oxygen
qPCR	Quantitative polymerase chain reaction
R_a	Rate of appearance
R_d	Rate of disposal
RNA	Ribonucleic acid
R-Primer	Reverse primer
RT	Reverse transcriptase
RT-PCR	Reverse transcriptase polymerase chain reaction
SDS	Sodium dodecyl sulfate
TE	Tris-ethylenediaminetetraacetic acid
USF-2a	Upstream stimulatory factor 2a

CHAPTER 1: GENERAL INTRODUCTION

1.1. Causes of environmental hypoxia in aquatic systems

Hypoxic events involve a decrease in the amount of available environmental oxygen (O_2), which can lead to stress, injury, or death for many animals. Hypoxia occurs in many bodies of water through natural means (Naqvi *et al.*, 2010; Williams *et al.*, 2019), and aquatic organisms are more likely to experience hypoxic conditions compared to terrestrial organisms due to the fact that water contains less O_2 than air. In open marine habitats, O_2 minimum zones experience hypoxia due to a combination of high O_2 demand (from increased nutrient availability) and slow O_2 renewal (Diaz & Rosenberg, 2008; Naqvi *et al.*, 2010). In coastal marine habitats and deep freshwater bodies, stratification of the water column can lead to hypoxia (Jenny *et al.*, 2016; Naqvi *et al.*, 2010). In shallow freshwater ecosystems, O_2 levels can vary over the course of the day, increasing during daytime due to active photosynthesis, and decreasing to hypoxic levels overnight (Williams *et al.*, 2019). While anthropogenic activity has increased the number of hypoxic events in both marine (Diaz & Rosenberg, 2008; Naqvi *et al.*, 2010) and freshwater (Jenny *et al.*, 2016; Williams *et al.*, 2019) systems, hypoxia and its effects tend to be more severe and widespread in freshwater environments (Jenny *et al.*, 2016).

The length and severity of hypoxic events can vary widely, with dissolved oxygen (DO) concentrations ranging from slightly hypoxic (~ 5 mg/L) (Carter *et al.*, 2021; Jane *et al.*, 2023) to severely hypoxic (~ 2 mg/L) (Carter *et al.*, 2021; Diaz & Rosenberg, 2008; Jane *et al.*, 2023) or near anoxic (<0.5 mg/L) ((Diaz & Rosenberg, 2008; Jane *et al.*, 2023). It can be difficult to differentiate between the effects of natural and artificial hypoxic events (Jenny *et al.*, 2016; Tellier *et al.*, 2022). Types of naturally occurring hypoxic events include hypolimnetic hypoxia, where summer stratification leads to the lower water layers in a lake being unable to replenish their O_2 levels; over-winter hypoxia, where layers of ice covering a lake reduce light penetration and by

extension photosynthesis rates as well as block O_2 renewal at the air-water interface; and diel hypoxia, where photosynthesis ceases at night and leads to a massive decrease in O_2 levels in the lake (Tellier *et al.*, 2022). However, the rates of naturally occurring hypoxic events are increasing in frequency due to climate change. Warming air temperatures are causing summer stratification to happen earlier and end later in the year (Jane *et al.*, 2023), and warmer water holds less O_2 while also increasing respiratory demand (Carter *et al.*, 2021; Strowbridge *et al.*, 2021). The main causes of artificial hypoxic events in lakes are large influxes of organic matter (Jane *et al.*, 2023; Jenny *et al.*, 2016; Tellier *et al.*, 2022). These can lead to algae blooms which use up large amounts of O_2 (Carter *et al.*, 2021; Jane *et al.*, 2023; Tellier *et al.*, 2022) and can also block light penetration, lowering photosynthesis rates in the process (Jane *et al.*, 2023). Depending on the circumstances, these types of hypoxic events can be acute, lasting for hours, or more chronic, lasting for days or weeks. Hypoxic events are expected to occur in increasingly unpredictable ways with climate change, meaning that the aquatic organisms could have more trouble acclimatizing to them (Tellier *et al.*, 2022).

1.2. Hypoxia tolerance in fishes

Tolerance to hypoxia varies widely between fishes. Fish that are more sensitive to hypoxia tend to have lifestyles that include long periods of sustained swimming, while more tolerant fish tend to be slower-moving or bottom-dwelling (Bickler & Buck, 2007). Examples of fish species exhibiting low hypoxia tolerance include salmonids like the freshwater rainbow trout (*Oncorhynchus mykiss*) (Dunn & Hochachka, 1986) or the anadromous Atlantic salmon (*Salmo salar*) (Davis, 1975), as well as marine tuna species like the skipjack tuna (*Katsuwonus pelamis*)

and yellowfin tuna (*Thunnus albacares*) (Bushnell & Brill, 1992). Freshwater fishes that are more tolerant to periods of hypoxia include freshwater cyprinids like the crucian carp (*Carassius carassius*) and domesticated goldfish (*Carassius auratus*), which maintain physical activity while exposed to seasonal hypoxia and anoxia (Cortes *et al.*, 2024; Nilsson, 2001); and tropical cichlid fishes like the Oscar (*Astronotus ocellatus*), which is exposed to frequent hypoxic conditions in the Amazon basin (Braz-Mota & Almeida-Val, 2021). Hypoxia-tolerant marine fishes include the short-horned sculpin (*Myoxocephalus scorpius*), a bottom-dwelling Arctic Ocean ambush predator (Jordan *et al.*, 2005; MacCormack & Driedzic, 2004).

1.3. Responses to hypoxia in fishes

While hypoxia responses in fish can vary widely, they can generally be distinguished into behavioural, physiological and molecular components. Their onset depends on the degree and duration of the exposure to hypoxia. Immediate responses to acute hypoxia include behavioural mechanisms such as avoidance of hypoxic areas in active species like the herring (*Clupea harenhus*) (Domenici *et al.*, 2013), aquatic surface respiration (ASR) demonstrated for European sea bass (Domenici *et al.*, 2013) and goldfish (Burggren, 1982). Physiological mechanisms include increased ventilation frequency and/or amplitude (Perry *et al.*, 2009, 2023), bradycardia (Vornanen *et al.*, 2009), and increased hematocrit levels (Craig *et al.*, 2014; García-Meilán *et al.*, 2022). In addition to the promotion of O_2 delivery, especially to highly aerobic tissues like the brain and heart, metabolic responses represent important components in the response to hypoxia (Johnston *et al.*, 2025). While the most efficient way to generate ATP is via aerobic (mitochondrial)

respiration, a switch to anaerobic respiration, or metabolic depression in highly hypoxia-tolerant organisms, serves to minimize O_2 use while maintaining reduced ATP production.

1.4. Molecular and epigenetic hypoxia-response pathways

Many of the physiological processes, including metabolic responses, are mediated, at least in part, at the gene expression level. The mechanistic research in fish aimed at linking molecular and physiological responses underlying hypoxia tolerance has focused primarily on the evolutionary conserved O_2 sensor 2-oxyglutarate-dependent prolyl hydroxylase (PHD), which has various isoforms (PHD1, PHD2, PHD3) that are coded by the Egl-9 family hypoxia inducible factor genes (*egln2*, *egln1*, and *egln3*, respectively) (Gerber *et al.*, 2024; Li *et al.*, 2023; Ma *et al.*, 2023). PHD (*egln*) activity is reduced under hypoxia (Li *et al.*, 2023), which leads to reduced hydroxylation of conserved proline residues in the transcription factor hypoxia-inducible factor 1α (HIF-1α), stabilizing it and allowing it to migrate to the nucleus, where it dimerizes with HIF-1β to produce HIF-1, which regulates the transcription of genes with hypoxia-response elements (HREs) (Greenald *et al.*, 2015; Mandic *et al.*, 2020, 2021).

In addition to this 'classical' molecular O_2 sensing pathway, different components of the epigenetic machinery, especially histone and DNA demethylases, have now emerged as being sensitive to hypoxia due to their dependence on O_2 (Johnston *et al.*, 2025). As such, these epigenetic pathways may directly regulate gene expression to contribute to physiological responses to hypoxia (Johnston *et al.*, 2025). For example, it has been reported that hypoxia exposure increases global DNA methylation in mammalian cell lines at near-anoxic conditions of ~1% O_2, in line with the reported low Michaelis constant (Km O_2 = ~30 μm) (Li *et al.*, 2023) and thus high

O_2 affinity of the ten-eleven translocation (TET) methyl cytosine dioxygenases, which act as erasers of DNA methylation (Thienpont *et al.*, 2016). The methylation of histones is another form of epigenetic control, relaxing or condensing chromatin to control access to DNA. The trimethylation of lysine 4 on histone 3 (H3K4me3) is a marker of relaxed chromatin, or euchromatin (Binda *et al.*, 2010). The trimethylation of H3K4 is catalysed by the lysine methyltransferase 2 (KMT2) family (Rao & Dou, 2015), while its demethylation is catalysed by the lysine demethylase 5 (KDM5) family (Batie *et al.*, 2019), with KDM5A having the strongest effects (Batie *et al.*, 2019; Johnston *et al.*, 2025; Li *et al.*, 2023). Specific increases in histone methylation marks associated with H3K4me3 have been shown to occur *in vitro* under more mild hypoxic conditions compared to TET enzymes (Batie *et al.*, 2019), in line with the reported higher Kms, and thus the lower O_2 affinities of the specifically involved demethylase KDM5A (Km O_2 = ~90 μM) (Li *et al.*, 2023). While the O_2 sensitivity of these epigenetic marks has been demonstrated to occur in a HIF-1α-independent fashion *in vitro*, the potential physiological role of epigenetic O_2 sensors remains unexplored *in vivo*.

1.5. Responses to acute hypoxia in rainbow trout

Rainbow trout have a lifestyle which includes long periods of extended swimming and has a higher metabolic rate compared to bottom-dwelling fish, making it more vulnerable to hypoxia (Haman *et al.*, 1997; Han *et al.*, 2022; Iftikar *et al.*, 2010; Svendsen *et al.*, 2012; Williams *et al.*, 2019). DO concentrations below 5 mg/L are considered acutely hypoxic for rainbow trout, and loss-of-equilibrium (LOE) has been shown to occur at 2 mg/L DO in this species (Han *et al.*, 2022). Under hypoxic conditions, many rainbow trout tissues switch to anaerobic glycolysis and increase

the production of lactate (Dunn & Hochachka, 1986, 1987; Omlin & Weber, 2010; Weber *et al.*, 2016), which is also observed in response to intense exercise (Omlin *et al.*, 2014; Teulier *et al.*, 2013; Weber *et al.*, 2016). Under hypoxic conditions, both lactate production and disposal are stimulated, with lactate disposal being stimulated to a lesser extent (Omlin *et al.*, 2014; Omlin & Weber, 2010; Weber *et al.*, 2016). White muscle is a major site of lactate production during both exercise and hypoxia (Dunn & Hochachka, 1986; Omlin & Weber, 2010, 2013; Weber *et al.*, 2016). Anatomically separate white muscle is used for short, high-speed swimming and is powered by anaerobic glycolysis, while lateral red muscle is used for sustained, low-speed swimming and powered by aerobic metabolism (Altringham & Ellerby, 1999; Gatz, 1973; Magnoni *et al.*, 2013; Weber, 2011). Red muscle, heart muscle, and the brain do not produce as much lactate as white muscle, but instead import and oxidise large amounts of it (Omlin & Weber, 2010, 2013). Under acutely hypoxic conditions, glucose turnover rates do not, or only transiently increase, while lactate turnover rates do. Much less is known about the regulation of lipid metabolism in rainbow trout tissues under acute hypoxia, although it is generally assumed that O_2 or ATP-intensive processes, such as beta-oxidation, are suppressed. If and how transcriptional responses contribute to favoring anerobic metabolism under acute hypoxia in rainbow trout tissues is currently less characterized, as is the potential role for O_2-sensitive epigenetic mechanisms in their regulation.

1.6. Objectives of the study and hypotheses

While there is a wide variation in the ability of fish to tolerate hypoxic conditions (Bickler & Buck, 2007; Rogers *et al.*, 2016), all animals exhibit physiological and molecular responses to hypoxia and a considerable amount of research has been done on those responses (Cerra *et al.*,

2023; Rogers *et al.*, 2016). However, there is a relative lack of knowledge on how cold-water fish that are sensitive to hypoxia, such as rainbow trout, respond to milder hypoxic events, anticipated to increase with climate change (Diaz & Rosenberg, 2008; Henson *et al.*, 2017; Jenny *et al.*, 2016; Pörtner & Knust, 2007). Rainbow trout are an economically and culturally important species with a near global distribution (Han *et al.*, 2022; Strowbridge *et al.*, 2021; Williams *et al.*, 2019), making them good models to understand how cold-adapted freshwater fish will be affected by expected increased occurrence of acute hypoxic events in their habitats. I am specifically interested in determining whether (i) specific thresholds for metabolic responses exist and are linked to circulating metabolite and/or tissue-specific or overarching gene expression changes linked to glucose, lactate, and lipid metabolism, and (ii) whether these changes are directly linked to hypoxia-responsive epigenetic marks involved in regulating transcription. I hypothesize that (i) metabolite and tissue-specific transcript changes support a preferential transcript level induction indicative of anerobic glucose and lactate utilization while inhibiting transcripts linked to fatty acid use and oxidation, and that (ii) this induction/repression coincides with O_2 sensitive histone modification marks linked to active and repressed promotors around the TSS, respectively. This project will provide novel mechanistic insight into the tissue-specific contributions of transcriptional changes of genes with critical roles in glucose, lactate and lipid metabolism in response to acute hypoxia exposures of different severity reflective of climate-change and explore the possible regulatory contribution of O_2-sensitive epigenetic marks at the transcriptional level. Together this work will expand our understanding of the effects of mild and severe hypoxia in aquatic, cold-adapted, freshwater, hypoxia-intolerant fishes and develop Chromatin immune-precipitation (ChIP) assays for use in non-traditional fish model species in a first effort to

comparatively probe the role of hypoxia-sensitive histone marks in the regulation of metabolic transcripts in fish species with different degrees of hypoxia tolerance.

CHAPTER 2: ACUTE HYPOXIA EXPOSURE REGULATES TRANSCRIPTS LINKED TO HEPATIC GLUCOSE AND LIPID METABOLISM AND THE PROMOTOR-SPECIFIC HISTONE MARK H3K4ME3 IN RAINBOW TROUT

2.1. Introduction

Environmental hypoxia occurs when DO in water falls below 2 mg/L, and severe hypoxia is defined as below 0.5 mg/L. Since fish gas exchange is driven by O_2 partial pressure (pO_2) gradients rather than absolute DO values directly, it is useful to use approximate conversions (Ultsch & Nordlie, 2019). At sea level and 13 °C, hypoxia corresponds to a pO_2 of <4 kPa (~20% saturation), and severe hypoxia to <1 kPa (~5% saturation). Recent studies highlight that hypoxia is becoming more common in freshwater systems like streams rivers, and lakes. A global survey found that 12.6% of rivers across 53 countries experienced hypoxic events. These events were typically short in duration (~3 h), and most likely to occur at night. Smaller rivers with warmer temperatures and slower flows were most at risk (Blaszczak *et al.*, 2023). A general and widespread increase in deoxygenation events in flowing rivers was identified in a study reconstructing daily DO concentrations in 580 rivers across the United States and 216 rivers in Central Europe by training a deep learning model (Zhi *et al.*, 2023). Deoxygenation was estimated to occur at a mean rate of −0.038 +/− 0.026 mg/L/decade, affecting 70% of the rivers. Projected future rates were estimated to exceed these historical rates by up to 2.5 times in 2100, indicating significant effects on river and stream water quality. Sediment records from 365 lakes show that since the mid-1800s, 20% have shifted to hypoxic conditions, mainly due to human-driven nutrient pollution (Jenny *et al.*, 2016). In over 400 lakes studied over 25 years, 75% showed longer stratification periods, leading to more frequent low-O_2 conditions during summer. During this time, an increase in deep water hypoxia by 0.9% - 1.7% per decade was estimated (Jane *et al.*, 2021). In the Great Lakes, more than 20 hypoxic zones have been documented, with the largest in Lake Erie's central basin. These zones vary in size and duration and are expected to grow with climate change, longer stratification, and increased nutrient runoff (Tellier *et al.*, 2022).

Freshwater teleost fishes, including commercially important aquaculture species, are expected to be exposed to increasing acute hypoxia events (Zhan *et al.*, 2023). The understanding of physiological and molecular responses to hypoxia are therefore important (Johnston *et al.*, 2025). Significant work on the physiologic responses to hypoxia has been done on rainbow trout, a freshwater species introduced to most continents (Muhlfeld *et al,* 2020). Rainbow trout are an important comparative research model, with economic importance as freshwater aquaculture and fishing species (Polakof & Moon, 2013). Rainbow trout are a highly active freshwater species considered comparatively hypoxia-intolerant. Indeed, compared to highly hypoxia-tolerant teleost species, such as the crucian carp and goldfish, rainbow trout exhibit an approximately ~2-fold higher P_{crit} of ~3 kPa at colder temperatures (5 - 19°C) (Rogers *et al.*, 2016; Ultsch *et al.*, 1980). Among the physiological responses to acute 3 - 4 h hypoxia exposure at described in rainbow trout are immediate metabolic responses of carbohydrate metabolism. Specifically, acute glycolytic activation in the muscle has been reported, likely using endogenous fuel to increase lactate turnover (Dunn & Hochachka, 1986, 1987; Omlin & Weber, 2010). Much less is known about acute changes to other aspects of intermediary metabolism, especially lipid and amino acid metabolism in trout and other fishes. The direct investigation of mechanisms involved in regulating transcriptional responses to acute hypoxia have historically been hampered by the lack of reliable antibodies to detect the evolutionarily highly conserved HIF-1α in teleost fishes (Mandic *et al.*, 2019). Under normoxia, Egl nine homolog (Egln) enzymes hydroxylate HIF-1α, which is then recognized by the Hippel Lindau factor to target it for degradation with extremely short half-life of <5 min (Semenza, 2004). Conversely, under hypoxia conditions, HIF-1α is stabilized and induces gene expression, including glycolytic metabolic genes, via nuclear binding to hypoxia response elements in the DNA (Semenza *et al.*, 1996). In absence of reliable antibodies for either

of the HIF-1 subunits in fish, the protein abundance of Egln (Gerber *et al.*, 2024) or the expression of its downstream target genes, have recently been used to quantify HIF-1α pathway activity under hypoxic conditions. Among these HIF-1α target genes is *egln3*, representing a feedback loop in the hypoxia sensing pathway. Indeed, *egln3* has been shown to be consistently induced under hypoxia in salmonids such as rainbow trout and Atlantic salmon (Kelly *et al.*, 2020; Liu *et al.*, 2017; Ma *et al.*, 2023), as well as cyprinids, such as goldfish and crucian carp (Cortes *et al.*, 2024), suggesting its suitability as molecular marker for the induction of the HIF-1α pathway under hypoxia. However, while *egln3* is useful as a singular marker, that fact that it represents a feedback loop in the HIF-1α pathway may make it difficult to distinguish between the contributions of hypoxia and HIF-1α on its induction or repression, so any attempts to separate the two should use multiple elements of the HIF-1α pathway.

While targeted quantification of transcripts coding for transporters and (rate-limiting) metabolic pathway components have demonstrated acute regulation in trout in response to nutritional stimuli (Jubouri *et al.*, 2021; Mennigen *et al.*, 2012; Talarico *et al.*, 2023) in line with important contributions of transcriptional-level regulation of intermediary metabolism (Desvergne *et al.*, 2006), such responses have remained comparatively less quantified until recently. With the availability of salmonid genomes of trout (Berthelot *et al.*, 2014; Lecomte *et al.*, 2025) and Atlantic salmon (Lien *et al.*, 2016), more detailed probing of transcript abundance at the paralogue resolution-level have become available. Indeed, experiments attempting to identify the possibility of developmental-hypoxia-dependent programming of intermediary metabolism in embryos (Liu *et al.*, 2017) have begun to characterize changes in putatively HIF-dependent glucose and lipid metabolism-related transcripts in embryos exposed to 20% O_2 saturation for 1 d. These studies revealed few changes in transcript abundance of transcripts involved in glucose and lactate

metabolism, apart from *mct4* induction (Liu *et al.*, 2017). Conversely, the effects of acute hypoxia on the regulation of transcript abundance with key function in lipid metabolism have not been investigated in separate tissues in adult rainbow trout.

In addition to allowing for more specific investigation of transcript changes at the paralogue-level, the availability of salmonid genomes of trout (Berthelot *et al.*, 2014; Lecomte *et al.*, 2025) and Atlantic salmon (Lien *et al.*, 2016) have also allowed for previously inaccessible probing of (putative) promotor regulation. In addition to the well-conserved O_2-dependent HIF-1α-dependent molecular signalling pathway (Semenza, 2004), more recent *in vitro* evidence suggests that parts of the epigenetic machinery may act as a direct O_2-sensors and regulators of gene expression (Li *et al.*, 2023). For example, O_2-dependent demethylases are involved in the dynamic regulation of histone modifications in a HIF-1α-independent fashion. This is exemplified by the reduced activity of lysine-specific demethylase 5A (KDM5A) under 1% hypoxia which stabilizes H3K4me3 marks known to mark the transcription start sites of active genes (Batie *et al.*, 2019). Similarly, reduced activity of KDM6A/UTX under hypoxia was shown to mediate stabilization of H3K27me3 marks associated with the downregulation of nearby genes via the formation of heterochromatic regions at 2% hypoxia (Chakraborty *et al.*, 2019). Finally, ten-eleven demethylases (TETs) were shown to be inhibited by 1 d exposure to 0.5% O_2, resulting in genome-wide hypermethylation of DNA (Thienpont *et al.*, 2016b). While these *in vitro* findings suggest direct O_2-dependent regulation of gene expression outside of the HIF-1α pathway, few studies have investigated this regulation and their contribution to transcriptional responses *in vivo,* including hypoxia-tolerant and -intolerant fishes (Farhat *et al.*, 2022; Johnston *et al.*, 2025).

Taking advantage of the sequenced and annotated rainbow trout genome (Berthelot *et al.*, 2014), the known rapid regulation of transcripts coding for key metabolite transporters and rate-

limiting enzymes (Jubouri *et al.*, 2021; Mennigen *et al.*, 2012; Talarico *et al.*, 2023), and the possibility to profile global and targeted transcriptional epigenetic regulation in the form of DNA methylation (Best *et al.*, 2024; Marandel *et al.*, 2016) and histone modifications (Marandel *et al.*, 2016; Liu *et al.*, 2017), we here investigate whether (i) acute hypoxia exposure affects intermediary metabolism to favour glucose over lipid utilization at the metabolite and tissue-specific transcript level, and whether (ii) transcript induction is specifically linked to O_2-sensitive epigenetic mechanisms, particularly H3K4me3 histone marks.

2.2. Materials and Methods

2.2.1. Animals

Adult rainbow trout (*Oncorhynchus mykiss*) were bought at the Linwood Acres trout hatchery (Campbellcroft, Ontario) and were allowed to acclimate for several weeks in a 1275 L flow-through fibreglass tank at 13°C in a 12L:12D photoperiod in the University of Ottawa Aquatics Facility. Tanks were supplied with flowing, aerated, 13°C dechloraminated tap water from the city of Ottawa. Rainbow trout were fed a diet of Skretting Orient Float feed each morning at a ratio of 1% of their body weight. All housing and experimental procedures were approved by the Animal Care Committee of the University of Ottawa (Protocol number: BL-3665) and adhered to the animal care guidelines for teaching and research established by the Canadian Council on Animal Care (CCAC).

2.2.2. Acute hypoxia exposure and tissue sampling

In the morning before the rainbow trout were fed, one random rainbow trout was collected from the 1275 L flow-through tank and placed in a blacked-out 15 L flow-through tank at 90%-

100% O_2 saturation (**Figure 1**). The order of assigned treatments was randomized, and retroactive comparison of morphometric parameters between treatment groups (n=10 for normoxia, 50% O_2 saturation, and 25% O_2 saturation) did not exhibit significant differences in body mass, fork length, or condition factor (**Table 1**). Under the normoxic treatment, the partial pressure of O_2 in the water was maintained at saturation level (pO_2=21 kPa) for 4 h. Under the 50% and 25% O_2 treatments, the O_2 was slowly lowered to 50% (pO_2=10.5 kPa) and 25% (pO_2=5.25 kPa) saturation respectively, over a period of 2 h and then maintained at that level for a following 2 h by bubbling N_2 through an equilibration column. Water pO_2 was measured using an OxyGuard Polaris C Dissolved Oxygen Meter (OxyGuard, Farum, Denmark). After 4 h, the trout was removed and left for 10 min in 60 mg/L bicarbonate-buffered MS-222 (pH=7). After terminal anesthesia was confirmed by non-responsiveness to pinching fins, measurements of mass, fork length, girth, and depth were taken, and blood was drawn via caudal vein puncture before the spinal cord was cut at the base of the skull. The fish was then dissected to collected liver, white and red muscle and adipose tissue (**Figure 1**). The tissues were wrapped in aluminum foil and immediately placed in dry ice. The blood was kept in regular ice before being spun at 12 000 × G for 12 min to separate the plasma. The plasma and tissues were stored at -80°C.

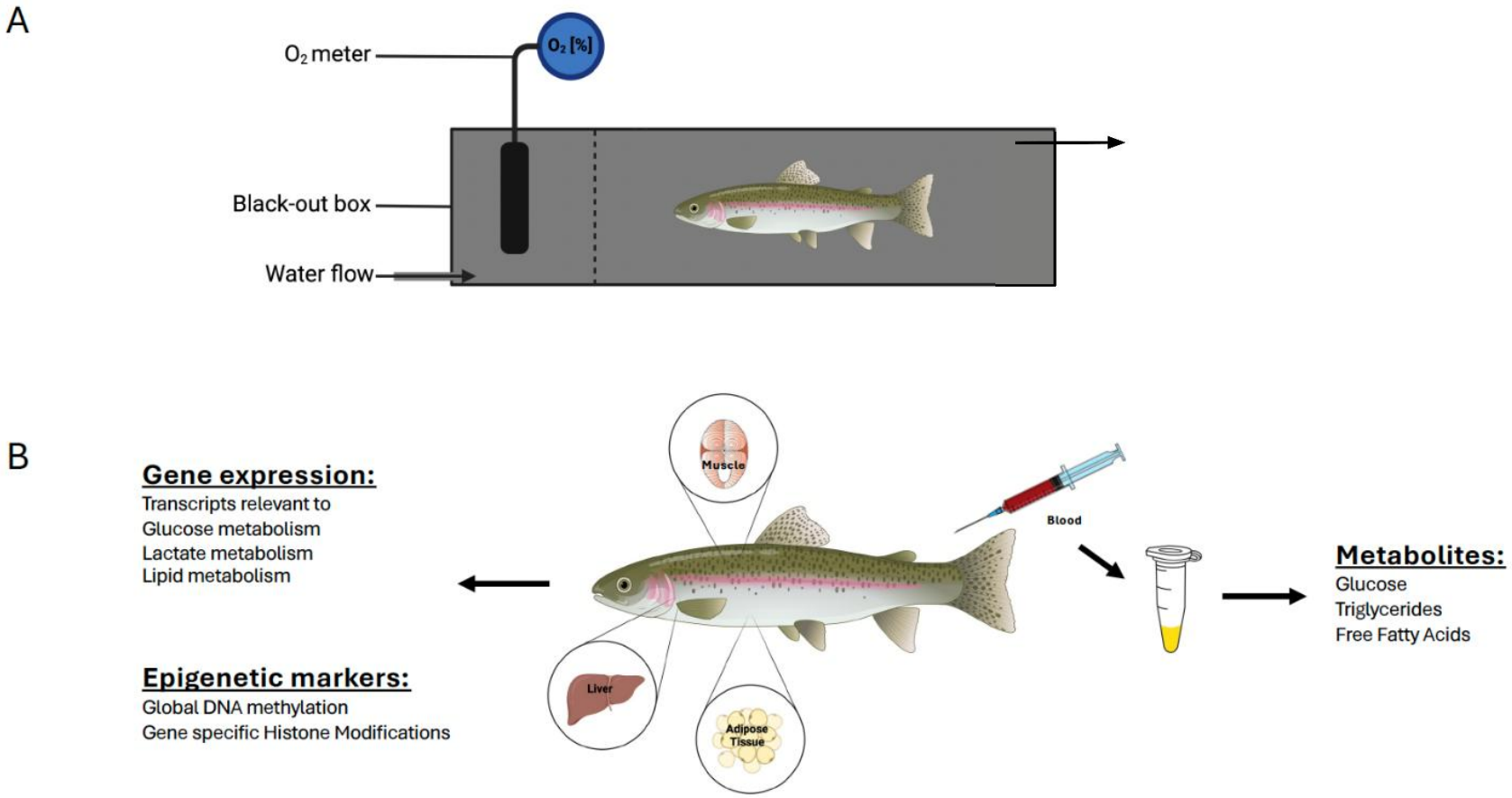

Figure 1. **(A)** Schematic representation of the experimental design and set-up and **(B)** overview of sampled tissues and quantified endpoints.

Table 1. Average morphometric parameters (+S.E.M.) of rainbow trout randomly placed in three experimental treatment groups (n=10/group). The condition factor (K) was calculated for each fish by dividing the mass (g) by the fork length cubed (cm^3) and multiplying it by 100 before averaging it for each treatment group. Sex was not correlated with any of the parameters measured and so both males and females were used in the analysis.

Parameter	**Normoxia**	**50% Hypoxia**	**25% Hypoxia**	**One-way ANOVA**
Body mass (g)	540.9 (±27.59)	513.7 (±47.27)	575 (±42.71)	df=2; F=0.62; *P*=0.55
Fork Length (cm)	35.49 (±0.57)	35.04 (±0.95)	35.79 (0.68)	df=2; F=0.24; *P*=0.78
Condition Factor (Fulton's K)	1.2 (±0.03)	1.16 (±0.04)	1.23 (±0.03)	df=2; F=1.1; *P*=0.35
Sex ratio F:M (%)	90	90	70	-

2.2.3. Plasma analyses

The Abbott Lite Blood Glucose Monitoring system (Abbot, Illinois, USA) was used to measure glucose levels in rainbow trout plasma, as it had been previously validated in zebrafish, *Danio rerio* (Eames *et al.*, 2010). The StatStrip Xpress Lactate system (Nova Biomedical, Waltham, MA, USA) was used to measure lactate concentrations in rainbow trout plasma as it had previously been validated in the Chinook salmon, *Oncorhynchus tshawytscha* (Vaage *et al.*, 2023). Each measurement was conducted on 5 µL plasma samples from each trout, and samples were run in duplicate. The Cayman Triglyceride Colorimetric Assay Kit (#10010303, Cayman Chemical, Ann Arbor, MI, USA) was used to measure plasma triglyceride levels using a spectrophotometric plate reader (Molecular Devices, San José, CA, USA). The Cayman Free Fatty Acid Fluorometric Assay Kit (#700310, Cayman Chemical, Ann Arbor, MI, USA) was used to measure plasma free fatty acid levels using a monochromatic fluorometer (Molecular Devices, San José, CA, USA). The DetectX® Cortisol ELISA Kit (Arbor Assay, Ann Arbor, MI, USA) was used to measure cortisol concentrations in rainbow trout plasma.

2.2.4. Realtime-RT PCR assays

2.2.4.1. RNA extraction and cDNA synthesis

Total ribonucleic acid (RNA) was extracted from liver, white muscle, red muscle, and adipose tissue from each trout by homogenizing 50 mg of tissue in 500 µL TRIzol™ reagent (Invitrogen, Burlington, Canada) using a Sonic Dismembrator model 100 (Fisher Scientific, Ottawa, ON, Canada) and separating the RNA with chloroform. The RNA pellet was dissolved in

DEPC water, quantified using a NanoDrop 1000 (Thermo-Fisher Scientific, Ottawa, ON, Canada), and stored at -80°C.

The QuantiTech Reverse Transcription Kit (#205313, Qiagen, Toronto, ON, Canada) was used to synthesize complementary deoxyribonucleic acid (cDNA) using total RNA from liver, white muscle, red muscle, and adipose tissue following the manufacturer's protocol. A no-reverse transcriptase (RT) negative control (RT replaced with RNAse-free water) was included to check for genomic contamination. The cDNA was stored at -20°C until used.

2.2.4.2. Primers

The relative steady state transcript abundance of genes with a wide variety of roles in HIF-1α, glucose and lactate metabolism, and lipid metabolism were quantified (**Figure 2**). To examine the molecular responses of the HIF-signaling pathway, the Egl 9 family hypoxia inducible factor 3 (*egln3*) was measured. To examine glucose metabolism, muscle glucose transporter type 4B (*glut4b*), the hepatic glycolytic enzyme glucokinase a (*gcka*) and the hepatic gluconeogenesis enzyme phosphoenolpyruvate kinase 1 (*pck1*) were quantified. To probe molecular regulation of components of lactate metabolism, lactate-transporting monocarboxylate transporters 1 (*mct1*) and 2 (*mct2*), and lactate metabolism enzymes lactate dehydrogenase A (*ldha*) and BB (*ldhbb*) were measured. To examine transcripts coding for key components of lipid metabolism, the intracellular fatty acid liberating enzyme hormone-sensitive lipase (*hsl*), the extracellular fatty-acid liberating enzyme lipoprotein lipase (*lpl*), the fatty acid importer fatty acid translocase (*cd36*), the fatty acid β-oxidation enzyme 3-hydroxyacyl-CoA dehydrogenase (*hoad*), and the fatty acid synthesis enzyme fatty acid synthase (*fasn*) were measured. The elongation factor 1α (*ef1α*) was used as a reference gene stably expressed between treatment groups (data not shown) to standardize the qPCR data analysis. The sequences of all primer pairs, NCBI gene ID, as well as their sources, if

applicable, are listed in **Table 2**. Newly designed Primers were generated using the freely available Primer3 software (https://primer3.ut.ee) using the following specifications: product size ranges between 100 and 300 bp, an optimal melting temperature of 60°C (range from 59°C to 61°C), a %GC content between 45% and 55%, a maximum self-complementarity of 4.00, and a maximum 3' self-complementary of 0.00. The gene sequences for the different isoforms were compared using the freely available Clustal Omega software (https://www.ebi.ac.uk/jdispatcher/msa/clustalo) to make sure that the primers were specific to a single isoform.

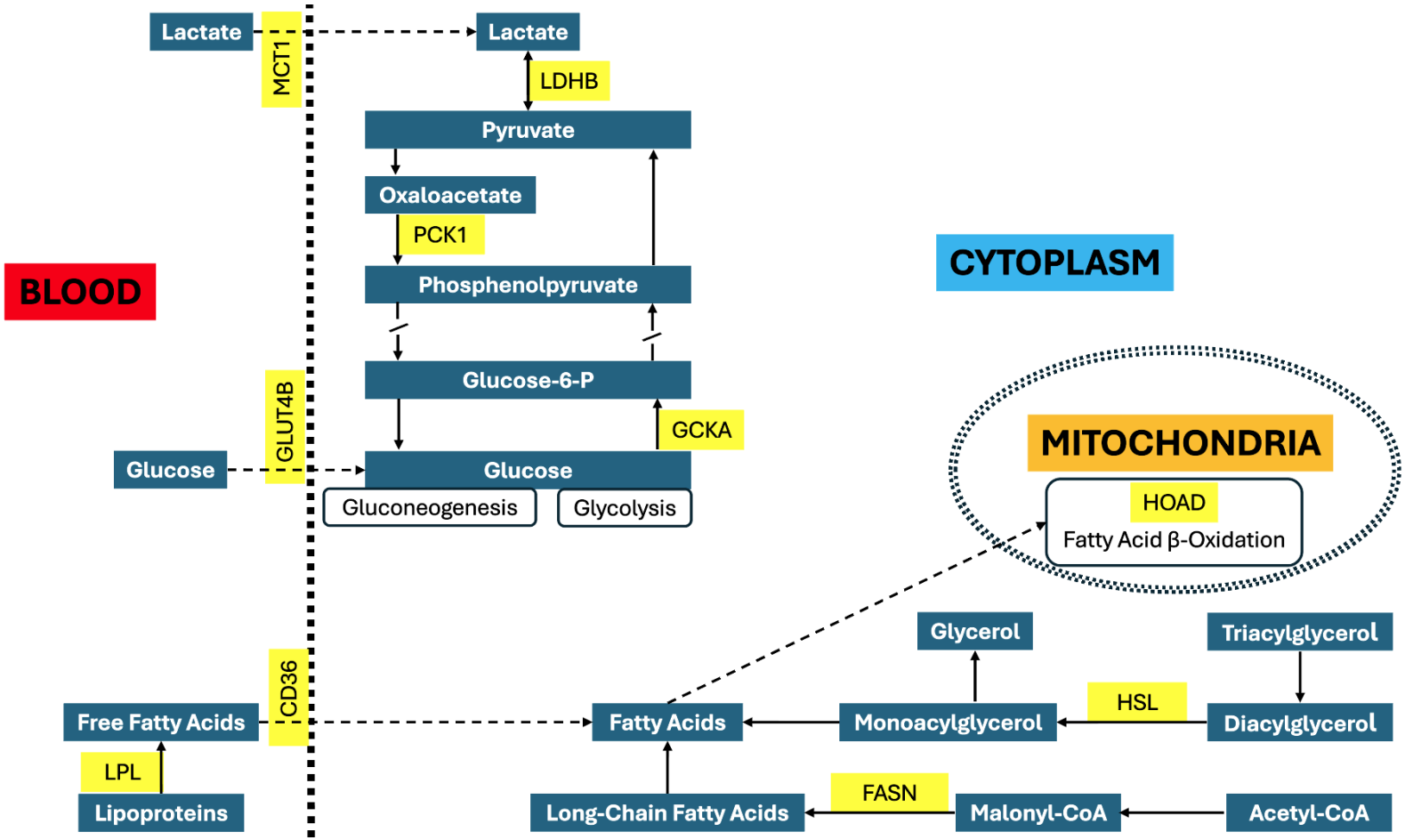

Figure 2. Generalized pathways for glucose, lactate, and fatty acid metabolism in rainbow trout. To examine glucose metabolism, muscle glucose transporter type 4B (*glut4b*), hepatic glucokinase a (*gcka*), and hepatic phosphoenolpyruvate kinase 1 (*pck1*) were quantified. To probe molecular regulation of components of lactate metabolism, lactate-transporting monocarboxylate transporters 1 (*mct1*) and 2 (*mct2*), and lactate dehydrogenase A (*ldha*) and BB (*ldhbb*) were measured. To examine transcripts coding for key components of lipid metabolism, hormone-sensitive lipase (*hsl*), lipoprotein lipase (*lpl*), fatty acid translocase (*cd36*), 3-hydroxyacyl-CoA dehydrogenase (*hoad*), and fatty acid synthase (*fasn*) were measured.

Table 2. Primer sequences, annealing temperatures and reaction efficiencies of specific SYBR-Green-based *real-time* RT-PCR assays measuring relative steady-state abundance of transcripts coding for proteins involved in O_2 sensing, and glucose-, lactate- and lipid-metabolism.

Gene Target	GenBank ID (NCBI) and Chromosome location	Primer Pair (5' - 3')	Amplicon Size (bp)	Tissue	Annealing Temperature (°C) Amplification Efficiency (%) Coefficient of determination (R^2)	Reference
egln3	110497687 (Chr. 19)	F: TAGCCTGGGTCAGTGGAGTT R: CACCATCGCCTTTGATCTTT	114	Liver Red Muscle White Muscle Adipose Tissue	61; 127.7; 0.956 61; 99.4; 0.977 61; 90.6; 0.905 61; 98.2; 0.985	This study
glut4b	110500678 (Chr. 21)	F: TCGGCTTTGGCTTCCAATATG R: GTTTGCTGAAGGTGTTGGAG	155	Red muscle White Muscle	57; 91.0; 0.975 57; 106.1; 0.982	Talarico et al., 2023 Jubouri et al., 2021
gcka	100135866 (Chr. 6)	F: CTGCCCACCTACGTCTGT R: GTCATGGCGTCCTCAGAGAT	237	Liver	54; 101.8; 0.964	Talarico et al., 2025
pck1	110493880 (Chr. 17)	F: ACAGGGTGAGGCAGATGTAGG R: CTAGTCTGTGGAGGTCTAAGGGC	97	Liver	55; 102.6; 0.991	Marandel et al., 2019 Kostyniuyk et al. 2019
ldha	110525514 (Chr. 1)	F: GACAAGGAGGACTGGAAGCA R: GGAACGCTGAGAAACACCTC	170	Red Muscle White Muscle	62; 97.0; 0.999 62; 103.3; 0.997	This study
ldhbb	110500268 (Chr. 21)	F: GTTTCCGTGCTAGGTGCTGT R: CCCCTCCCTTTGTTTCTTTC	145	Liver Red Muscle White Muscle Adipose Tissue	63; 99.0; 0.979 62; 104.0; 0.984 62; 95.6; 0.991 62; 90.2; 0.925	This study
mct1	110494698 (Chr. 17)	F: GAAGATGCTGCCAAGGAGAG R: CACAAAGGCCAGAACAGACA	218	Liver Red Muscle	62; 90.4; 0.955 62; 98.8; 0.957	This study
mct2	110500080 (Chr. 21)	F: CTGCCACCAAGAAGAAGGAG R: CCCGACAGGTAGATGAGGAA	103	Adipose Tissue	60; 100.5; 0.980	This study
hsl	100505413 (Chr. 23)	F: TGCCTTCCTGTACTCGCAAG R: GCAAGAAAGGCAAGGGTGTT	134	Liver Red Muscle White Muscle	56; 98.9; 0.937 57; 103.6; 0.989 56; 104.7; 0.945	Kostyniuk et al., 2019

lpl	100136622 (Chr. 5)	F: ACATGAGCCGGAAAGAGAAA R: GGTTGGGAGGCAGAACATAC	201	Liver Red Muscle White Muscle Adipose Tissue	60; 94.7; 0.984 60; 102.8; 0.976 60; 104.1; 0.973 59; 95.9; 0.994	Talarico et al., 2025
cd36	100136247 (Chr. 11)	F: GATTCTCTGCGCCCATCTAC R: GGGTTCTTCCACGACTCAAA	137	Liver Red Muscle	60; 98.5; 0.987 60; 93.8; 0.947	Talarico et al., 2025
hoad	110497328 (Chr. 19)	F: GGACAAAGTGGCACCAGCAC R: GGGACGGGGTTGAAGAAGTG	125	Liver Red Muscle White Muscle	60; 95.2; 0.968 60; 96.5; 0.994 60; 92.4; 0.989	Talarico et al., 2025
fasn	110499230 (Chr. 20)	F: TGATCTGAAGGCCCGTGTCA R: TATGGTGCGTTGCAGTGGG	161	Liver Adipose Tissue	58; 96.8; 0.983 58; 106.2; 0.993	Kostyniuk et al., 2019

2.2.4.3. Real-time RT-PCR

All *real-time* RT-PCR assays were conducted using a CFX96 Opus™ (Bio-Rad, Mississauga, ON, Canada) system and CFX Manager™ Software. The total reaction volume for each qPCR reaction was 20 µL, which consisted of 1 µL each of 10 nM specific forward and reverse primers (**Table 2**; IDT, Coralville, IA, USA), 7 µL of DEPC water, 10 µL of SsoAdvanced Universal SYBR Green Supermix (Bio-Rad), and 1 µL of diluted cDNA template. Each *real-time* RT-PCR assay was run with the following cycle parameters: a 30 s activation step at 95°C, 40 cycles consisting of a 5 s denaturation step at 95°C and a 5 s annealing and extension step at the primer-specific temperature (**Table 2**). For all SYBR-Green based *real-time* RT-PCR assays, the no-RT negative control was included to control for genomic contamination. Following each run, melting curves were generated by gradual increases in incubation temperatures from 65°C to 95°C at a rate of 0.5°C increase / 5s, and loss of fluorescence was monitored to confirm single peaks indicative of single, homogeneous amplicons. For each assay a serially diluted standard curve and individual samples were run in duplicates. Average values of samples with <0.5 dCT difference was retained. Standard curves with efficiencies between 90-110% representing a doubling of relative amplicon abundance with each cycle were deemed acceptable, as were R^2 values >0.96. Following all transcript-specific *real-time* RT-PCR assay runs, CT threshold values were normalized to CT threshold values of the reference gene *ef1α*, and subsequently normalized to control group using the ddCT method (Livak & Schmittgen, 2001) for each tissue.

2.2.5. Analysis of epigenetic marks

2.2.5.1. Total DNA extraction and global DNA methylation quantification

Total deoxyribonucleic acid (DNA) was extracted from liver from each trout using the DNeasy Blood and Tissue Kit (#69506, Qiagen, Toronto, ON, Canada) following the manufacturer's instructions. Samples were stored at -80°C.

The MethylFlash Global DNA Methylation (5-mC) ELISA Easy Kit (P-1030-96, EpigenTek, East Farmingdale, NY, USA) was used to measure total DNA methylation in liver DNA from each trout following the manufacturer's instructions. Absorbance readings were taken using a spectrophotometric plate reader (Molecular Devices, San José, CA, USA) at 450 nm. Absorption values were converted to % 5-mC DNA using the standard curve.

2.2.5.2. ChIP assays

Chromatin immunoprecipitation (ChIP) DNA was extracted from liver from 4 trout exposed to each treatment (n=12). Fifty milligrams of each tissue was incubated using 1% methanol-free formaldehyde in 500 µL PBS (Sigma-Aldrich, Oakville, ON, Canada) and Roche cOmplete Protease Inhibitor Cocktail (#4693116001, Roche/Sigma-Aldrich) and the chromatin was sheared using a Bioruptor® Plus (Diagenode, Liége, Belgium). To create the ChIP aliquots, Magna ChIP™ Protein G Magnetic Beads (#16-662, Merck-Millipore, Burlington, MA, USA), ChIP dilution buffer, and either the H3K4me3 antibody (#C15410003, Diagenode), the H3 antibody (ab1791, Abcam, Waltham, MA, USA) or the IgG antibody (#C15410206, Diagenode) were added to the sheared DNA. The next day, the immune complexes were washed with low-salt (20 mmol/L Tris pH 7.4, 0.1% SDS, 1% Triton X-100, 2 mmol/L EDTA, 150 mmol/L NaCl), high-salt (20 mmol/L Tris pH 7.4, 0.1% SDS, 1% Triton X-100, 1 mmol/L EDTA, 500 mmol/L

NaCl), LiCl (10 mmol/L Tris pH8, 1% NP-40, 1% Sodium Deoxycholate, 1 mmol/L EDTA, 0.25 mol/L LiCl), and TE (10 mmol/L Tris pH 7.4, 1 mmol/L EDTA) buffers before they were extracted using TE buffer with 1% SDS and proteinase K (# 3115828001, Roche/Sigma-Aldrich) and heating in a dry bath at 65°C for 2 h and then 95°C for 10 min. The DNA was then purified using the EZ-10 Spin Column PCR Products Purification Kit (#BS664, BioBasic, Markham, ON, Canada) and amplified with PCR in using GoTaq Green Master Mix (Promega, Madison, WI, USA).

2.2.5.3 Assessment of H3K4me3 histone marks upstream of hypoxia-induced metabolic gene transcripts

Primers were designed to detect specific DNA fragments from the putative promotor regions 2000 bp upstream of TSS of 2 genes (*pck1*, *mct1*). These genes were chosen because their transcripts showed robust and significant induction following exposure to the 25% hypoxia treatment in liver tissue, and because *pck1* had previously been investigated and validated in rainbow trout liver ChIP assays (Marandel *et al.*, 2016). Primer pairs for upstream *mct1* DNA fragments were designed using Primer3 using previously described parameters. The *mct1* primers were validated by amplifying them from sheared chromatin in a standard PCR and resolving them by amplicon size in a 1% Agarose gel (**Figure 3**). Following validation and optimization of efficiency (90-110%) and R^2 values (>0.96), qPCR reactions were run as previously described, with the exception that 1 µL of sheared chromatin input / ChIP assay DNA templates were used. The run through a qPCR with the following cycle parameters: a 30-second activation step at 95°C, 40 cycles consisting of a 5-second denaturation step at 95°C and a 5-second annealing and extension step at the primer-specific temperature. For all analysis PCR runs, a no-RT negative control was included in each assay to control for genomic contamination. The ChIP data were

analyzed by the ‘percent input’ method, in which 1% starting chromatin is used and ChIP CT values are divided by input (=total chromatin) derived values. H3K4me3 values were then normalized to H3 values to obtain ratio changes, and all data was then normalized to normoxic control ratios. The list of primer sequences and specific PCR conditions is provided in **Table 3**.

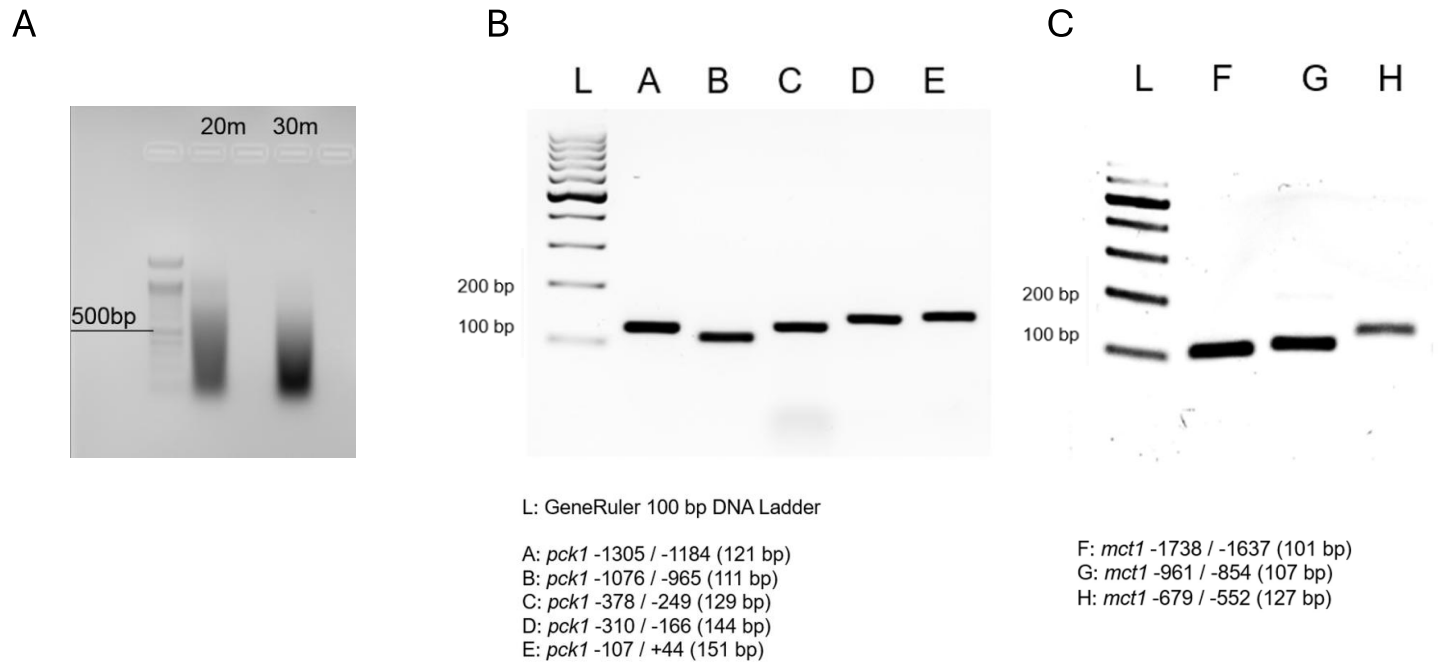

Figure 3. DNA visualized using the SYBR Safe gel stain following 1% Agarose gel electrophoresis. **(A)** Incubation time-dependency of chromatin shearing efficiency under the described Bioruptor™ shearing protocol parameters. (**B**) DNA amplicons obtained from PCRs using a sheared Chromatin template to probe DNA regions upstream of TSS of *pck1* and *mct1* genes.

Table 3. Primer sequences, annealing temperatures and reaction efficiencies of SYBR-Green-based *real-time* ChIP-PCR targeting specific sequences in putative promoter sequences upstream of the TSS of the *pck1* and *mct1* genes involved in glucose- and lactate-metabolism.

Gene Target	GenBank ID (NCBI) and Chromosome location	Location from Transcription Start Site (TSS)	Primers (5'-3')	Amplicon size (bp)	Annealing Temperature (°C) Amplification Efficiency (%) Coefficient of determination (R^2)	Reference
pck1	110493880 (Chr. 17)	-1305 / -1184	F: TGGCCAAGTCAAAGTCCAGA R: CCCATTCCTCCTTGCAAAACA	121	60 104.2 0.98	Marandel et al., 2016
		-1076 / -965	F: GCTGAATAATTTTGCACGCCC R: AGAATCAACAACAAGTGGGACA	111	60 98.2 0.97	
		-378 / -249	F: TCAAGGATCGGCACATTCCT R: AGTGATTCAACAGTTTCGCTCT	129	60 92.7 0.94	
		-310 / -166	F: GCCTCCAAAATGTGCCAATAG R: CAACTGAGCATCTTGTTCTTTCA	144	60 105.4 0.98	
		-107 / +44	F: CAGAGTTTTCCAAGAGCTGAACA R: GGGCTGTTCTTGAATTGTATCCA	151	60 114.3 0.95	
mct1	110494698 (Chr. 17)	-1738 / -1637	F: GTGGTCCCCTACAAGGAATG R: AGGGCTTGGGAAAGGAAA	101	59 98.4 0.96	This study
		-961 / -854	F: GCTGTGATGATGTGGTGCTT R: CAGCAGTCAGGGTCATTTCTT	107	59 88.4 0.98	
		-679 / -552	F: CCCTTTTGGAACCCTTTTTC R: ACATCATCCCCTCCCAGTT	127	60 107.5 0.97	

2.2.6. Statistical Analysis and Data Visualization

Prism Version 10 (Graphpad Software, La Jolla, CA, USA) were used for all data analysis and visualization of all individual metabolite, gene expression and ChIP assay data and their correlations. Briefly, data were tested for the assumption of normal distribution for each treatment group using the Shapiro-Wilk normality test. In cases data were non-parametric, standard transformations were used to meet the normality criteria. Data were then investigated for outliers using the Grubb's method, and one-way ANOVAs run. In cases of significance of the omnibus test ($P<0.05$) a Tukey's post-hoc test was run for results with equal variances (assessed by Brown-Forsythe test). In cases data were not homoscedastic, a Welch's ANOVA and Dunnett's multiple comparison's tests were run. If one or more of the treatment groups could not be normalized following transformation, a non-parametric Kruskal-Wallis test was run ($P<0.05$) and, in cases of significant differences ($P<0.05\%$) differences between specific treatment groups resolved by post-hoc tests. Correlations between metabolites and transcript abundance were calculated using Pearson correlations and heatmap visualization. Nipal's Principal Component Analysis (PCA) was computed using row vector scaling in the open software Clustal Vis (Metsalu & Vilo, 2015). Heatmaps were generated in Clustal Vis using centering of rows.

2.3. Results

2.3.1. Graded acute hypoxia does not induce HIF-1α responsive egln3 transcript across tissues

The experimental set-up successfully created normoxia and graded hypoxia exposure conditions (**Figure 4A**), as indicated by a significant treatment (between factor) × time (within-factor) interaction in a repeated measure ANOVA without the assumption of sphericity and the

application of a Geisser-Greenhouse correction (df=24; F=57.33; P<0.0001). Following a gradual reduction over the first 2 h before maintaining final saturation levels of 50% O_2 and 25% O_2 over 2 h respectively, O_2 saturation levels of both hypoxia treatment groups were significantly lower compared to normoxia at and after 20 min (P<0.05), and significantly different not only compared to normoxia, but also each other for all timepoints measured after 1 h and thereafter (P<0.05). Gene expression of the proposed hypoxic marker gene *egln3* (**Figure 4B**) was not significantly different between treatment groups in liver (df=2; H=1.54; *P*=0.48), white muscle (df=2; F=0.9 *P*=0.42), red muscle (df=2; F=1.44; *P*=0.26), and adipose tissue (df=2; F=0.53 *P*=0.60).

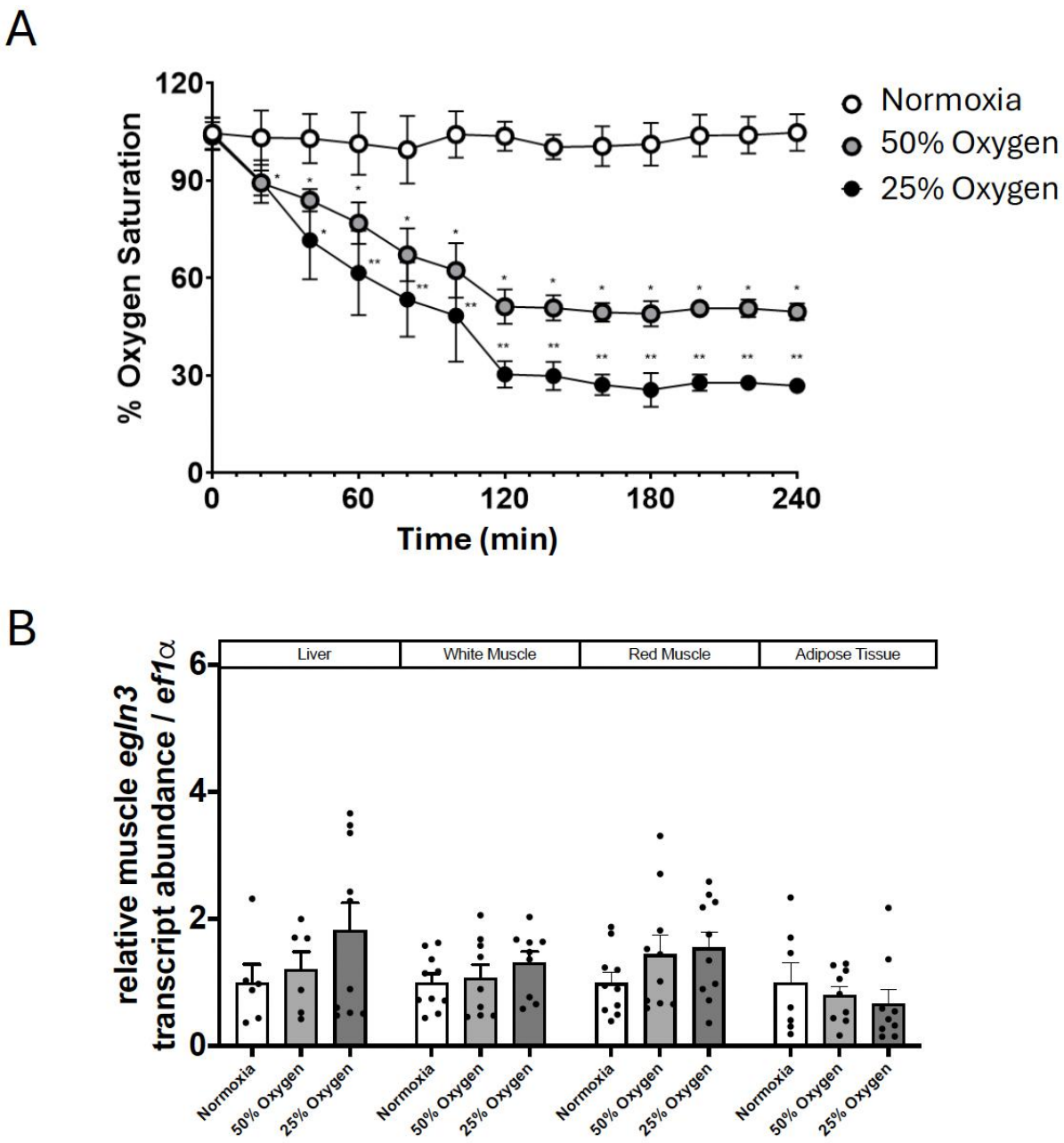

Figure 4. (A) Partial pressure of O_2 (pO_2) measurements expressed as % O_2 saturation taken from N_2 infused dechloraminated system flow-through water in the exposure tank at 20 min intervals over the 4 h duration of the experiment (A). In this set-up, adult rainbow trout were exposed to normoxia (n=10), 50% O_2 saturation hypoxia (n=10), and 25% O_2 saturation hypoxia (n=10). Average measure ± S.E.M. are shown. Repeated measurement data were tested for normal distribution and sphericity and analyzed by repeated measurement one-way ANOVA with applied Greenhouse-Geisser correction. Significant treatment*time interactions were resolved by timepoint-specific post-hoc comparisons ($P<0.05$). Time-point-specific significant differences in O_2 saturation from normoxic controls are indicated by a single asterisk (*) and differences between hypoxia treatment groups and control are indicated by a double asterisk (**).

(B) Relative steady-state transcript abundance of the HIF-1α regulated molecular hypoxia marker *egln3*. Individual and treatment group average data (± S.E.M.) of *egln3* transcript abundance normalized to *ef1α* are shown. All data were normalized to average normoxic control group data to depict relative-fold changes in transcript abundance. Data were tested for normal distribution and homoscedasticity and analyzed using a one-way ANOVA when these conditions were met, and by Kruskal-Wallis in cases were data or transformed did not meet these criteria. In cases of significant differences ($P<0.05$) of the omnibus test, significant differences between treatment groups were resolved by post-hoc analysis ($P<0.05$).

2.3.2. Acute hypoxia exposure does not significantly alter steady-state concentration of circulating oxidative fuels compared to normoxic controls while inducing hypoxia stress markers

There were no significant differences between treatment groups for the plasma concentration of glucose (df=2; F=2.646; *P*=0.089), triglycerides (df=2; F=2.16; *P*=0.4), or free fatty acids (df=2; F=0.4356; *P*=0.65) There was a significant increase in levels of plasma lactate (df=2; F=10.68; *P*=0.0001) and cortisol (df=2; F=4.43; *P*=0.03) between the normoxia group and the highest level of hypoxia exposure (**Figure 5**).

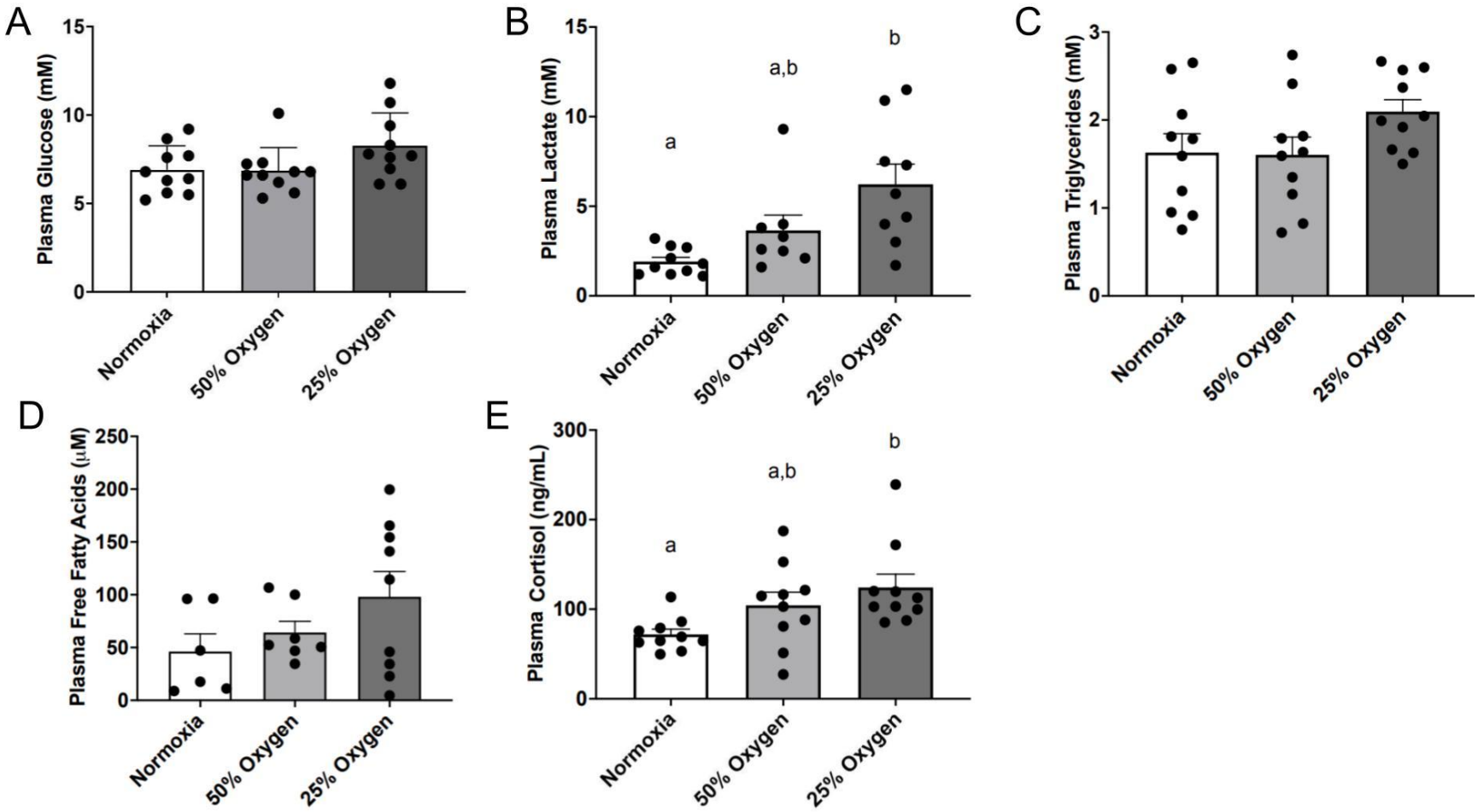

Figure 5. Plasma metabolite concentrations of **(A)** glucose, **(B)** lactate, **(C)** triglycerides, **(D)** free fatty acids, and **(E)** cortisol sampled from adult rainbow trout exposed to normoxia (n=10), 50% O_2 saturation hypoxia (n=10) and 25% O_2 saturation hypoxia (n=10) for a period of 4 h. Individual and treatment group average data (± S.E.M.) are shown. Significant differences (P<0.05) between treatment groups are indicated by different letters.

2.3.3. Changes in transcript abundance reveal tissue-specific transcriptional regulation of carbohydrate, lactate and lipid metabolism

The targeted analysis of transcripts with roles in metabolism revealed that the highest number of hypoxia-treatment induced changes (n=6) occurred in the liver. Regarding hepatic glucose metabolism, transcripts coding for the glycolytic enzyme Gck1 (**Figure 6A;** df=2; F=7.025; P<0.01), and gluconeogenic enzyme Pck1 (**Figure 6B;** df=2; F=20.72; P<0.01) were induced at both levels of hypoxia exposure (P<0.05) and the highest level of hypoxia exposure (P<0.01), respectively. Of the transcripts coding for proteins with roles in hepatic lactate metabolism, the transporter *mct1* was induced at both levels of hypoxia exposure compared to normoxic controls (**Figure 6C**; df=2; F=4.08; *P*=0.03), while the transcript for the lactate dehydrogenase isoform b (*ldhbb*) remained unchanged by hypoxia exposure compared to normoxic controls (**Figure 6D**; df=2; F=0.27; P=0.77).With regard to hepatic lipid metabolism, transcripts coding for the intracellular fatty-acid liberating enzyme Hsl (**Figure 6D**; df=2; F=9.65; P<0.01), the fatty-acid importing transporter CD36 (**Figure 6E**; df=2; F=5.61; P=0.01) and the fatty acid synthase Fasn (**Figure 6F**; df=2; F=8.17; P<0.01), but not the β-oxidation enzyme Hoad (**Figure 6G**; df=2; F=2.40; P=0.12), were significantly induced by the highest level of hypoxia compared to other treatment groups (P<0.05).

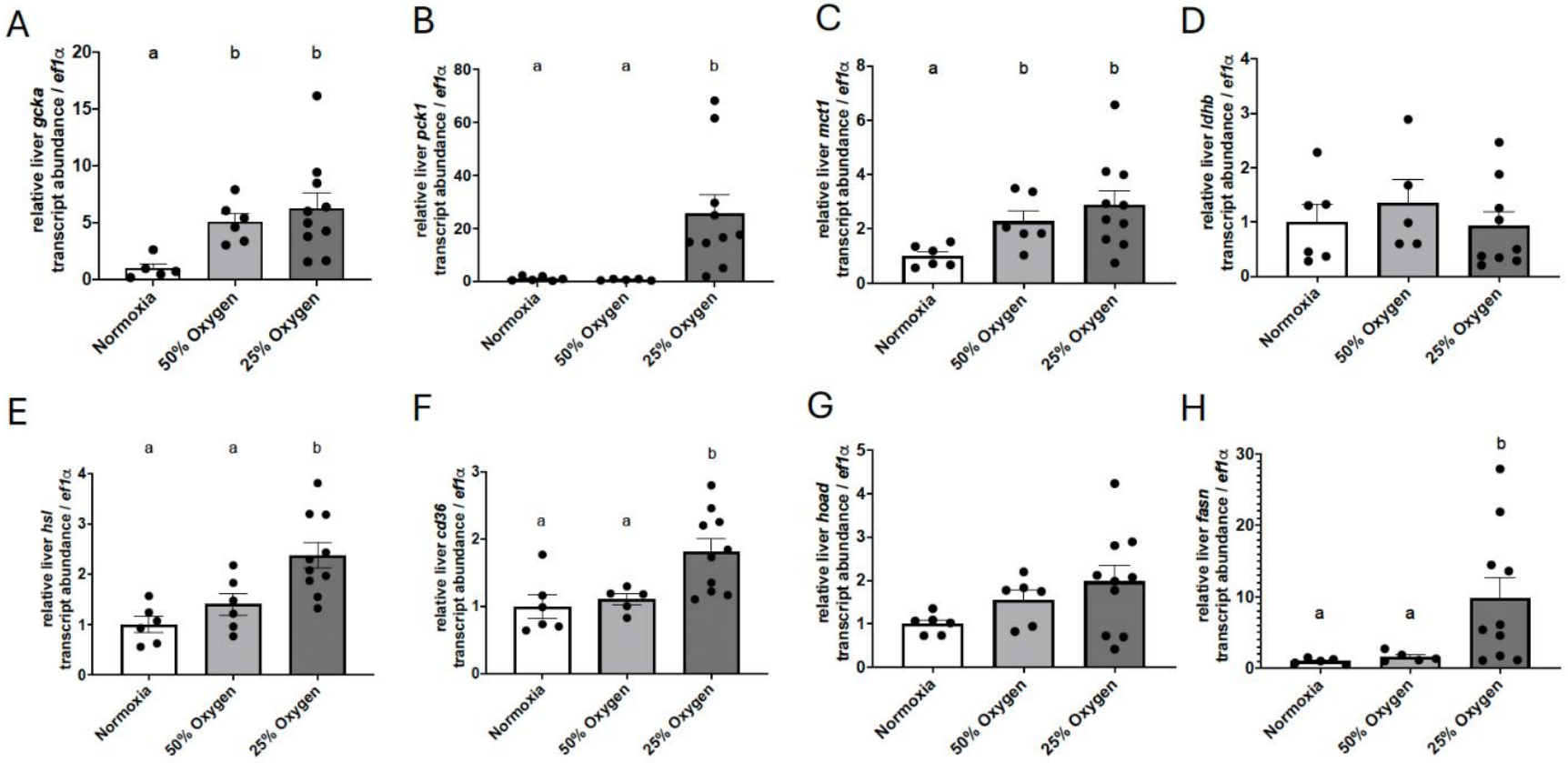

Figure 6. Relative steady-state transcript abundance of hepatic transcripts related to glucose (**A-B**), lactate (**C-D**), and lipid metabolism (**E-H**). Individual and treatment group (n=10) average data (± S.E.M.) of transcript abundance normalized to *ef1α* are shown. All data were normalized to average normoxic control group data to depict relative-fold changes in transcript abundance. Significant differences (P<0.05) between treatment groups are indicated by different letters.

Hypoxia exposure resulted in the induction of several transcripts in white muscle (n=3) and red muscle (n=1) tissue compared to normoxic controls. Regarding transcripts coding for proteins involved in muscular glucose and lactate metabolism (**Figure 7A-C**), the abundance of *glut4b* transcripts, coding for paralogues of the glucose transporter 4 increased significantly ($P<0.05$) in the 25% O_2 saturation group compared to normoxic controls in white muscle (df=2; F=4.33 $P<0.02$), but not red muscle tissue (df=2; F=2.60; $P=0.09$). Conversely, no changes in the transcript abundance of lactate dehydrogenase isoforms *ldha* (white muscle df=2; F=0.10; $P>0.05$ / red muscle: df=2; F=1.91; $P>0.17$) and *ldhbb* (white muscle: df=2; F=0.41; $P=0.67$ / red muscle df=2; F=0.59; $P=0.56$) were observed). Regarding transcripts coding for components involved in muscular lipid metabolism (**Figure 7D-G**), the abundance of transcripts of the fatty acid importer *cd36* (white muscle: df=2; F=5.56; $P=0.01$ / red muscle: df=2; F=1.77; $P=0.19$) and the extra-cellular fatty acid-liberating enzyme Lpl (white muscle: df=2; F=3.87; $P=0.04$ / red muscle: df=2; F=3.9; $P=0.03$) were significantly increased in the 25% O_2 saturation group over normoxic controls ($P<0.05$) in white and red muscle, respectively. Conversely, transcript abundance of neither *hsl* (white muscle: df=2; F=2.24; $P=0.13$ / red muscle: df=2; F=3.52; $P=0.05$), nor *hoad* (white muscle: df=2; F=0.76; $P=0.47$ / red muscle: df=2; F=0.34; P=0.72) were significantly affected by treatments.

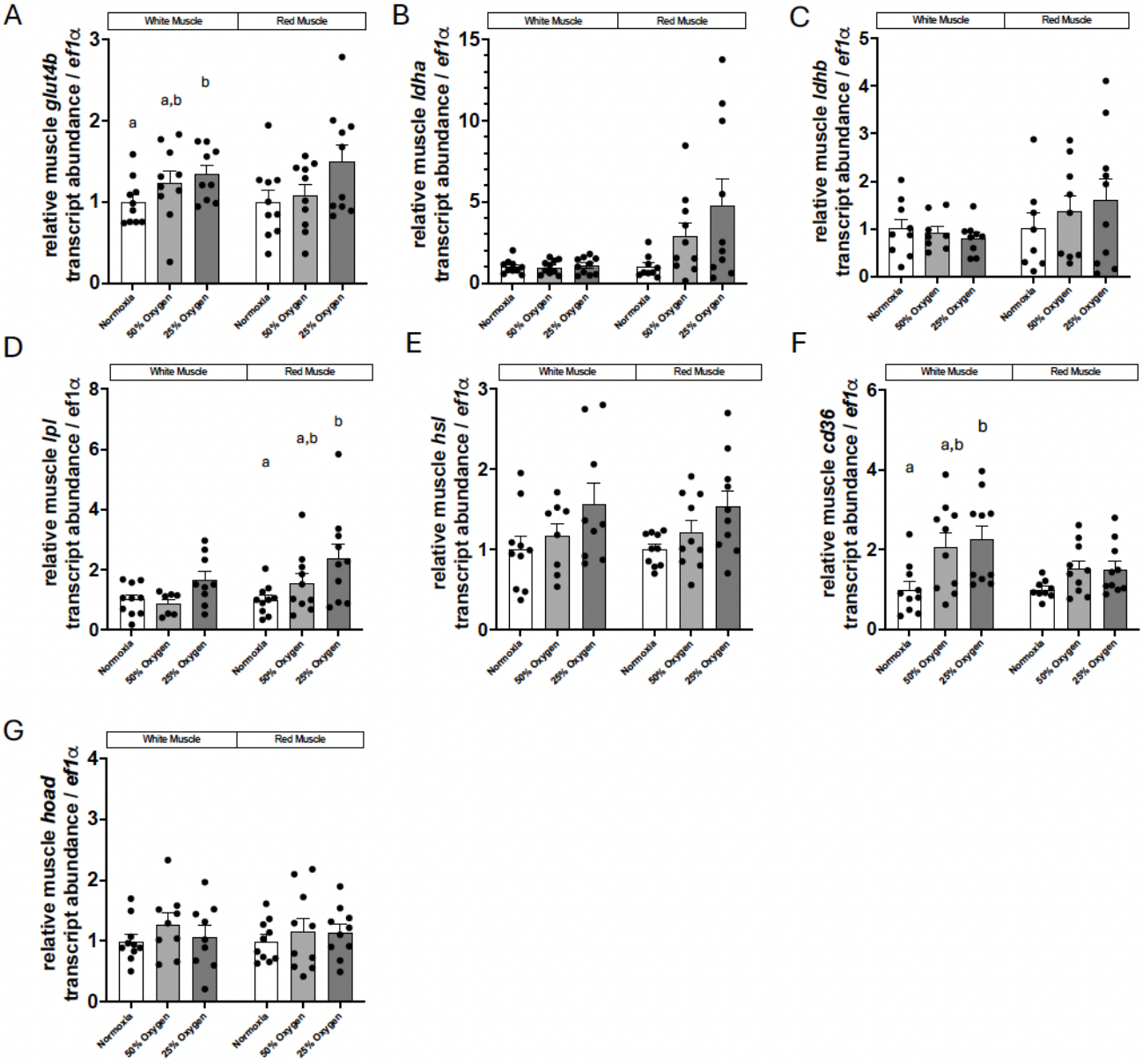

Figure 7. Relative steady-state transcript abundance of white and red muscle transcripts related to glucose (**A**), lactate (**B-C**), and lipid metabolism (**D-G**). Individual and treatment group (n=10) average data (± S.E.M.) of transcript abundance normalized to *ef1α* are shown. All data were normalized to average normoxic control group data to depict relative-fold changes in transcript abundance. Significant differences (P<0.05) between treatment groups are indicated by different letters.

In adipose tissue, two transcripts were significantly affected by hypoxia treatments. Regarding transcripts coding for components of glucose and lactate metabolism (**Figure 8A-B**), the lactate importer *mct2* (df=2; F=3.82; *P*=0.04) but not lactate producing *ldhbb* (df=2; H=1.04; P=0.60) were affected by hypoxia treatment, with a significant induction at the highest level of hypoxia compared to normoxia in the former (*P*<0.05). Considering lipid metabolism, the transcript abundance of *lpl*, coding for the extracellular lipolytic enzyme LPL, (**Figure 8C**; df=2; F=5.42; *P*=0.02) was induced by the highest hypoxia exposure group (*P*<0.05), while no change was observed in the *fasn* transcript (**Figure 8D**; df=2; F=2.39; *P*=0.13).

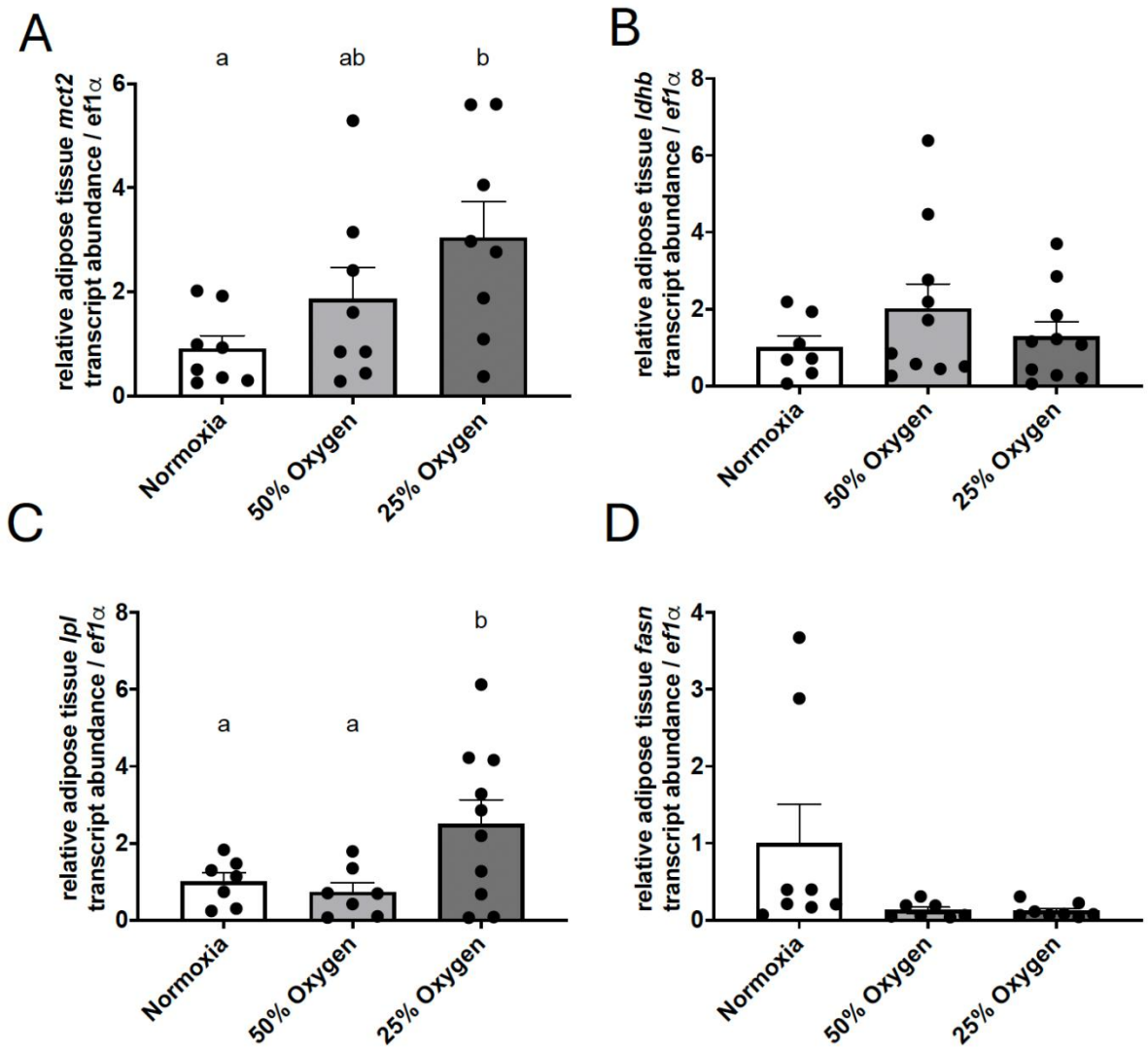

Figure 8. Relative steady-state transcript abundance of adipose tissue transcripts related to lactate **(A-B)** and lipid metabolism (**C-D**). Individual and treatment group (n=10) average data (± S.E.M.) of transcript abundance normalized to *ef1α* are shown. All data were normalized to average normoxic control group data to depict relative-fold changes in transcript abundance. Significant differences (P<0.05) between treatment groups are indicated by different letters.

2.3.4. Acute hypoxia does not affect hepatic global DNA methylation, but specifically alters H3K4me3 histone marks upstream of pck1 and mct1 TSS

While no difference between overall percentage of 5-mC DNA/total DNA were observed in liver tissue (**Figure 9**; df=2; F=0.4; P=0.67), we did observe significant differences in H3K4me3/H3 ratios in upstream sequences of the *pck1* (**Figure 10A**), but not *mct1* (**Figure 11A**) gene. Specifically, significant decreases in H3K4me3/H3 ratios upstream of the *pck1* gene (**Figure 10B**) were detected in response to both 50% ($P<0.01$) and 25% ($P<0.05$) O_2 saturation compared to normoxic controls for the DNA fragment extending from bp -1305 to -1184 upstream of the TSS (df=2; F=19.87; $P<0.01$), and in response to 50% O_2 saturation ($P<0.01$) for the DNA fragments extending from bp -1076 to -965 (df=2; F=19.14; $P<0.01$). No significant changes were observed for the ratios at fragments extending from fragment bp -378 to -249 (df=2; F=3.01; $P=0.16$), bp -310 to -166 (df=2; 1.44; $P=0.29$) and bp -107 to +44 (df=2; F=2.13; $P=0.2$). There were no significant changes in the ratios of H3K4me3/H3 upstream of the *mct1* gene TSS (**Figure 11B)** for the fragments spanning bp -1738 to -1637 (df=2; F=3.16; $P=0.12$), bp –961 to -854 (df=2; F=1.09; $P=0.44$).

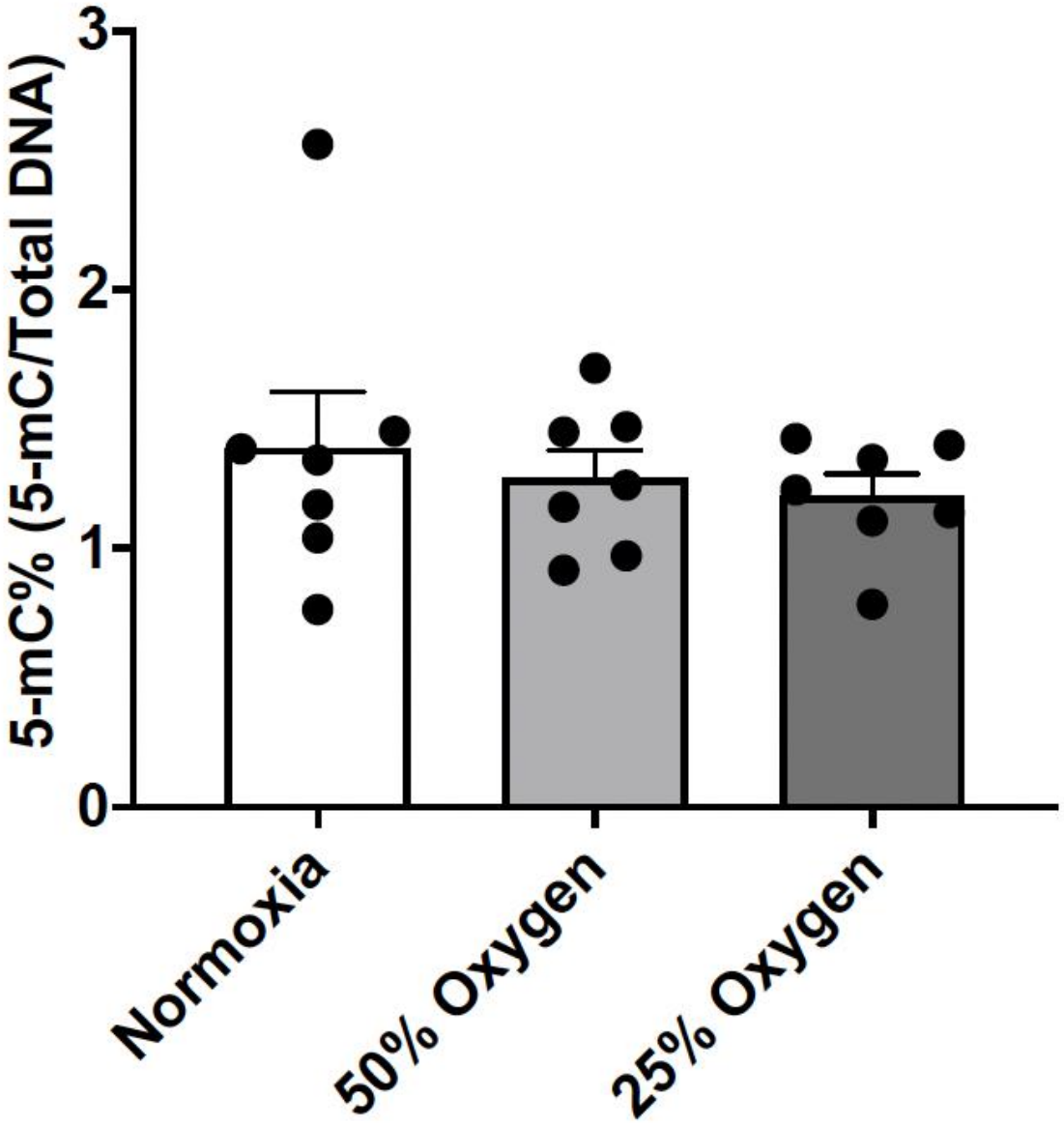

Figure 9. Hepatic epigenetic mark analysis of total DNA methylation (5-mC) expressed as % total DNA.

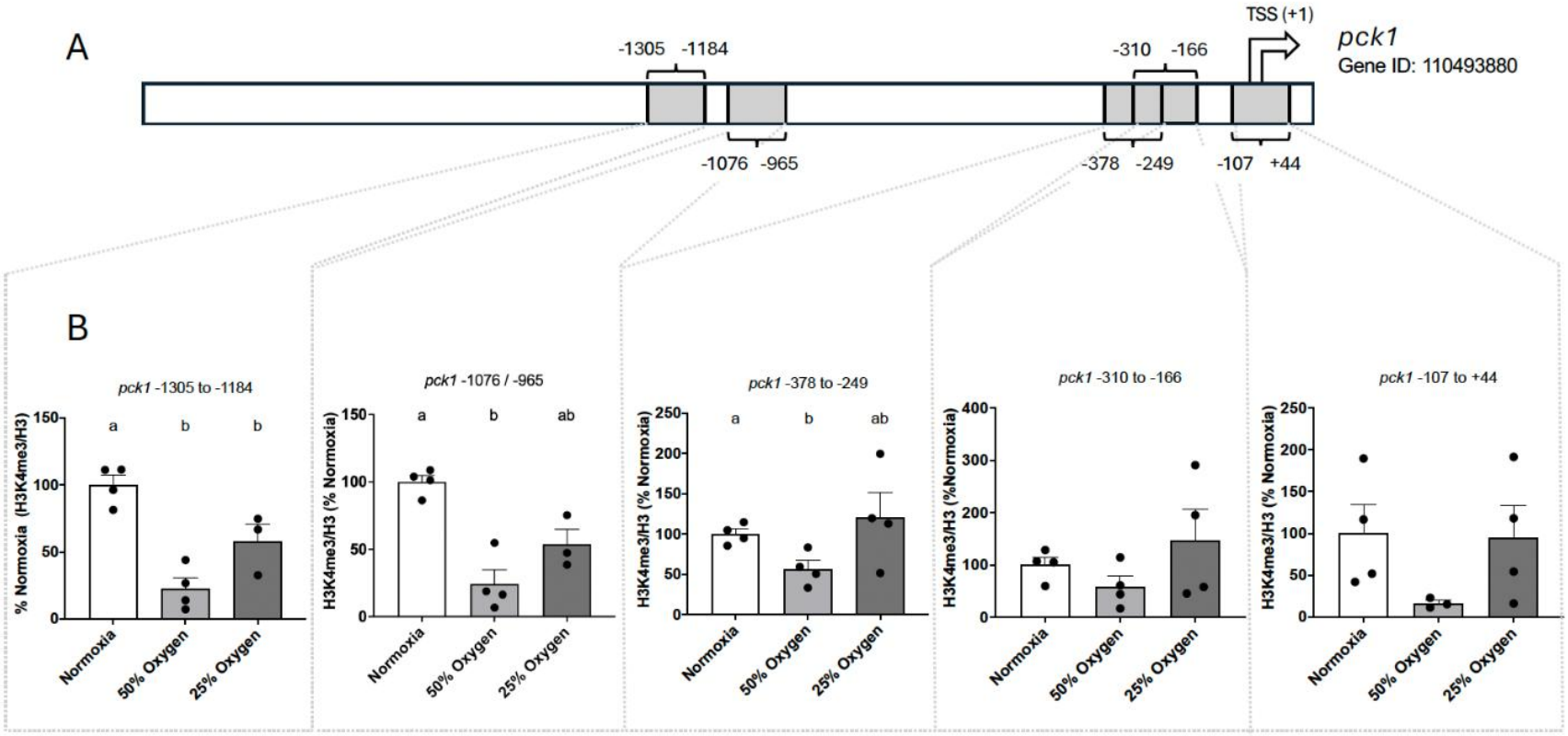

Figure 10. H3K4me3/H3 occupancy of hepatic DNA fragments of the putative upstream promoter sequences of upstream up to 2000 bp of the TSS of *pck1*. **(A)** Location of DNA fragments profiled in ChIP assays. (**B**) Individual and group average (n=4) specific H3K4me3/H3 enrichment normalized to input and normoxic control group to illustrate fold-change. Significant differences (P<0.05) between treatment groups are indicated by different letters.

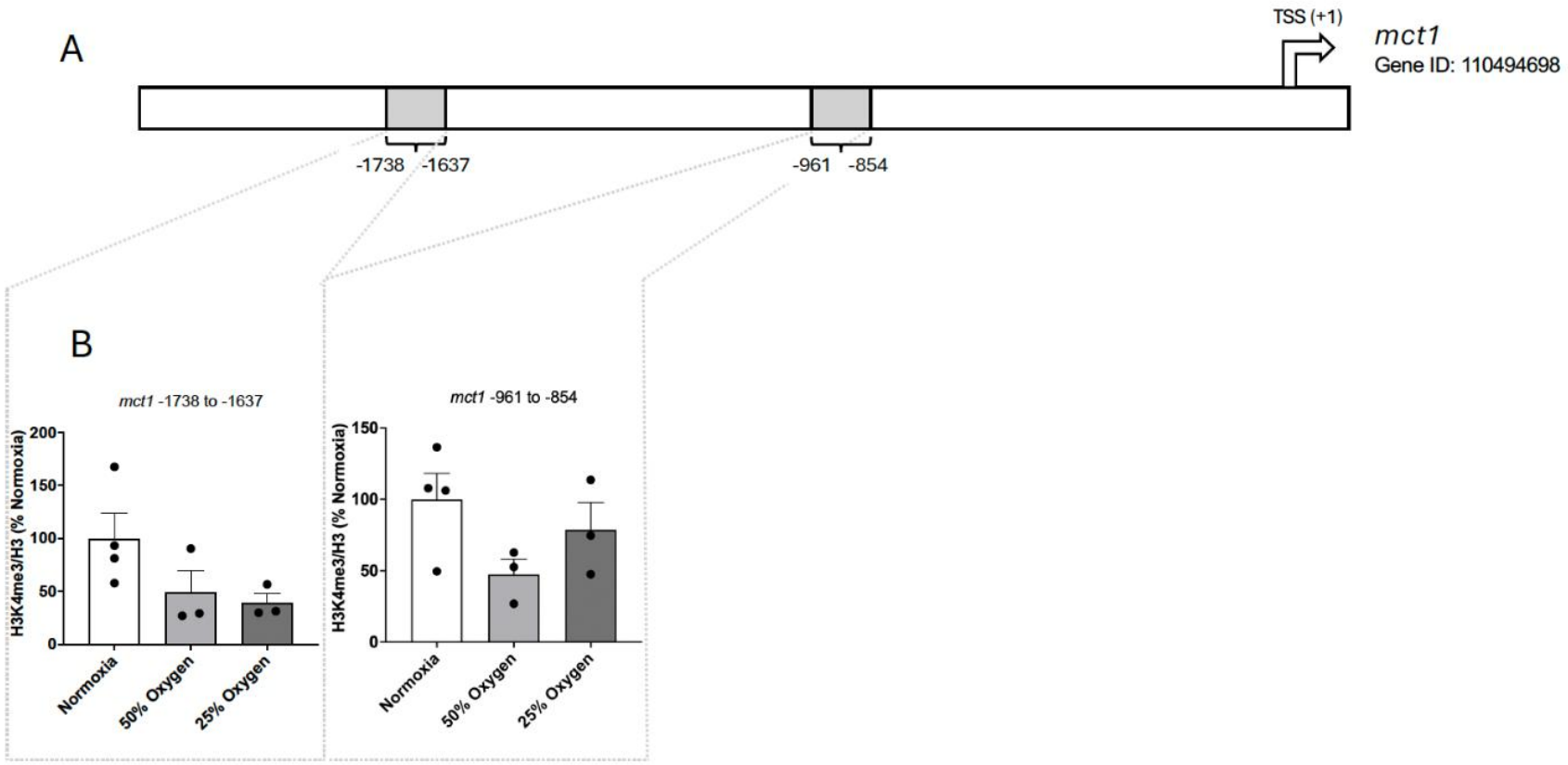

Figure 11. H3K4me3/H3 occupancy of hepatic DNA fragments of the putative upstream promoter sequences of upstream up to 2000bp of the TSS of *mct1*. **(A)** Location of DNA fragments profiled in ChIP assays. (**B**) Individual and group average (n=4) specific H3K4me3/H3 enrichment normalized to input and normoxic control group to illustrate fold-change.

2.3.5. Correlational analyses suggest H3K4me3 is not linked to induction of pck1 and mct1 transcript abundance following acute hypoxia exposure

Correlational analyses between hepatic H3K4me3/H3 ratios in individual upstream DNA fragments of *pck1* genes in the putative promoter region (2000 bp upstream of TSS) and the hepatic *pck1* transcript abundance, respectively, revealed a general lack significant Pearson correlation for most within-individual comparisons in all comparisons, with the exception of a strong positive correlation between upstream DNA fragment bp -310 to -166 H3K4me3/H3 and *pck1* transcript abundance (r=0.8; $P<0.05$). No significant Pearson correlation coefficients were identified between DNA fragments within the putative promoter region of *mct1* and *mct1* transcript abundance.

2.3.6. Measured circulating metabolite and tissue-specific transcript abundance data does not allow to fully distinguish individuals between exposure groups

To assess whether hypoxia-dependent transcript changes correlate between tissues and with circulating metabolites, a global Pearson-correlation table was created and visualized in the form of a heatmap **(Figure 12).** Global Pearson correlations between transcript in all tissues and circulating metabolites revealed examples of coordinated expression of metabolites and tissue-specific transcripts, transcripts within a specific tissue, and transcripts across different tissues. For example, circulating glucose showed the strongest significant correlation with hepatic *pck1* transcript abundance (r=0.56; $P<0.01$), while high degrees of within- and to some extent between-tissue correlation of transcripts linked to free fatty acid transport and metabolism could be observed. In the liver, for example, the expression of free fatty acid producing extracellular *lpl*, intracellular *hsl*, the free fatty acid importer *cd36*, and the β-oxidation enzyme *hoad* were significantly correlated (r=0.44; $P<0.05$). Transcript abundance of *hsl* was significantly correlated

between all tissues where it was measured (liver, red muscle, white muscle; r=0.52; P<0.01). Several significant and strong correlations were also observed between transcripts belonging to different metabolic pathways. When using Nipal's PCA on vector scaled-row data metabolite and tissue-specific transcript abundance data, 25.3% and 12.6% of the variation on Principal Component 1 and 2, respectively (**Figure 13**). When rows and columns are clustered using correlation distance and average linkage for heat-map visualization, no complete separation of hypoxia treatment group samples from each other or normoxia group samples is observed (**Figure 14).**

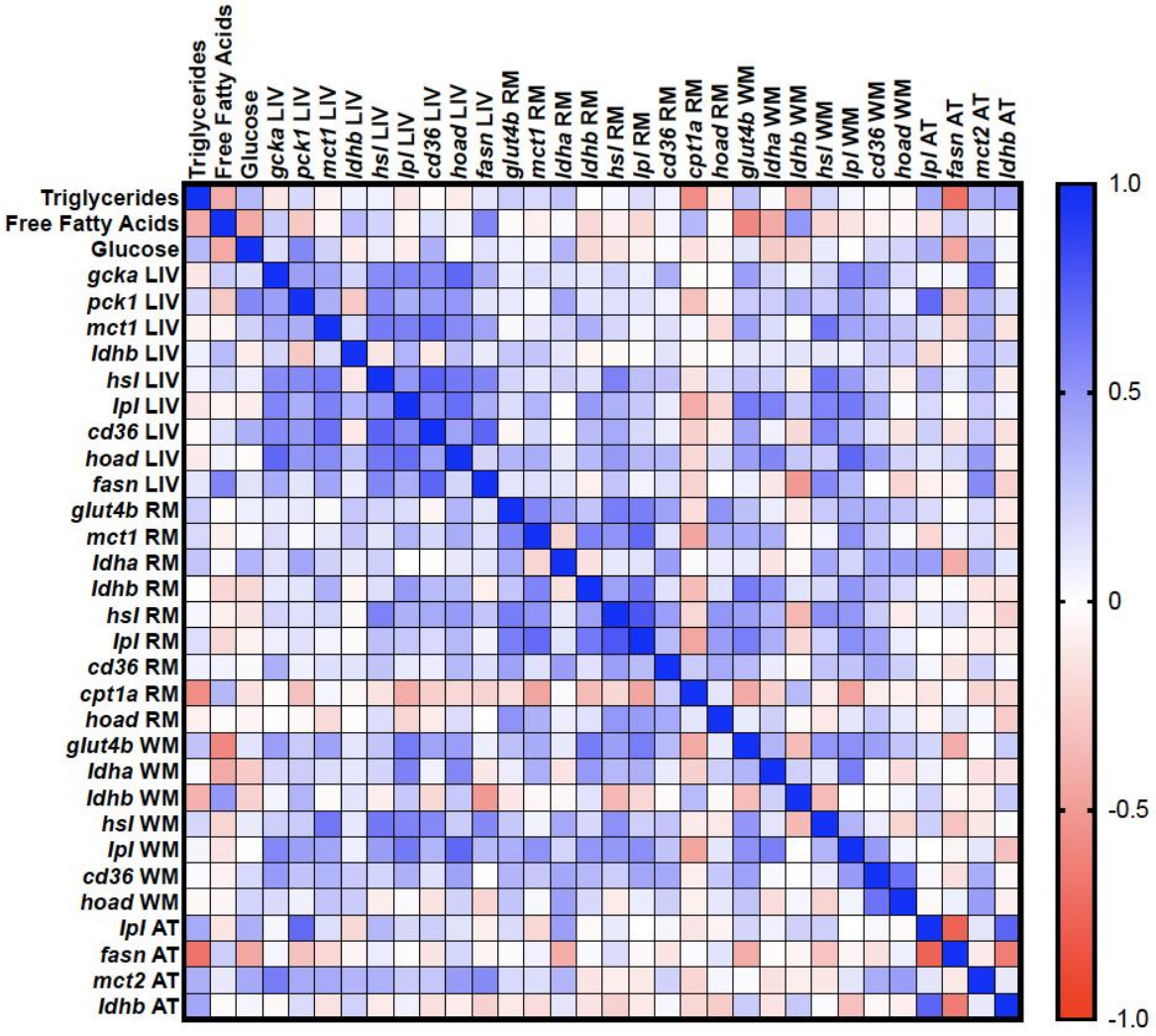

Figure 12. Heatmap of Pearson correlations for all measured tissue-specific transcripts and circulating metabolites.

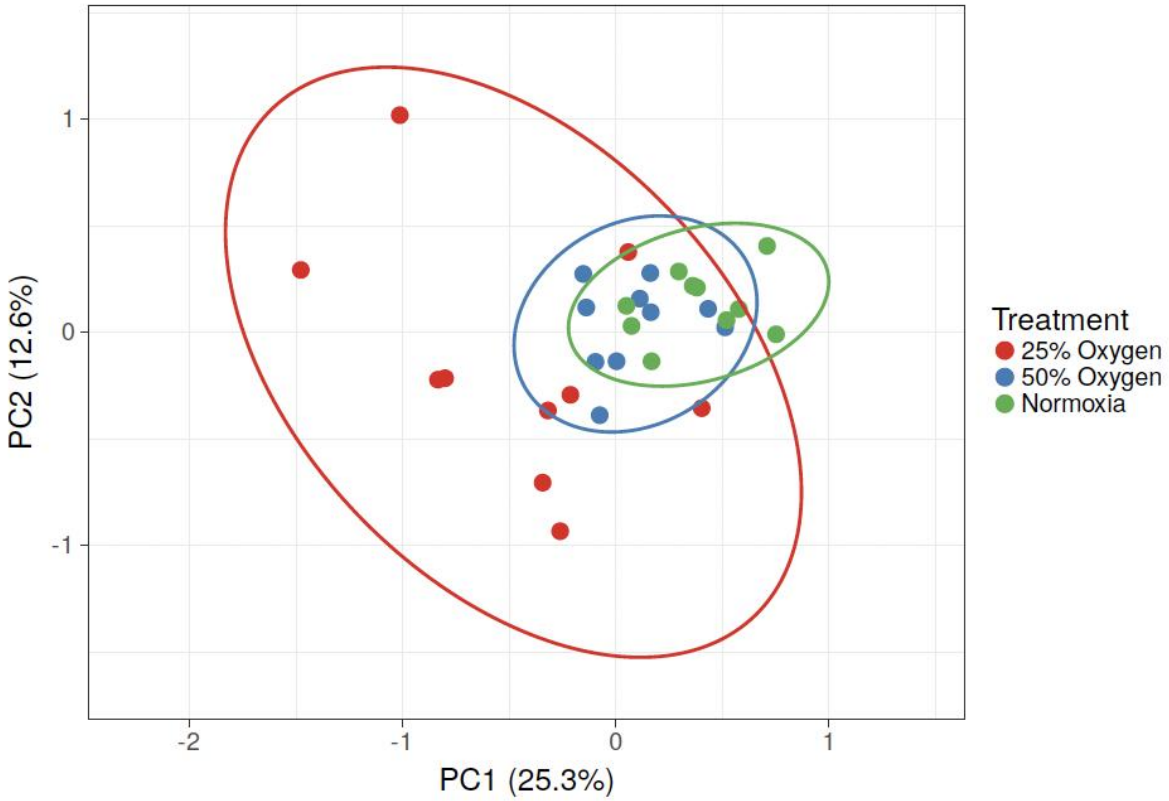

Figure 13. Nipal's Principal Component Analysis of vector-scaled individual (n=10 per treatment group) transcript and metabolite data. X and Y axis show Principal Component 1 and 2 that explain 25.3% and 12.6 of the total variance, respectively. Prediction ellipses are such that with probability 0.95, a new observation of the same group will fall inside the ellipse.

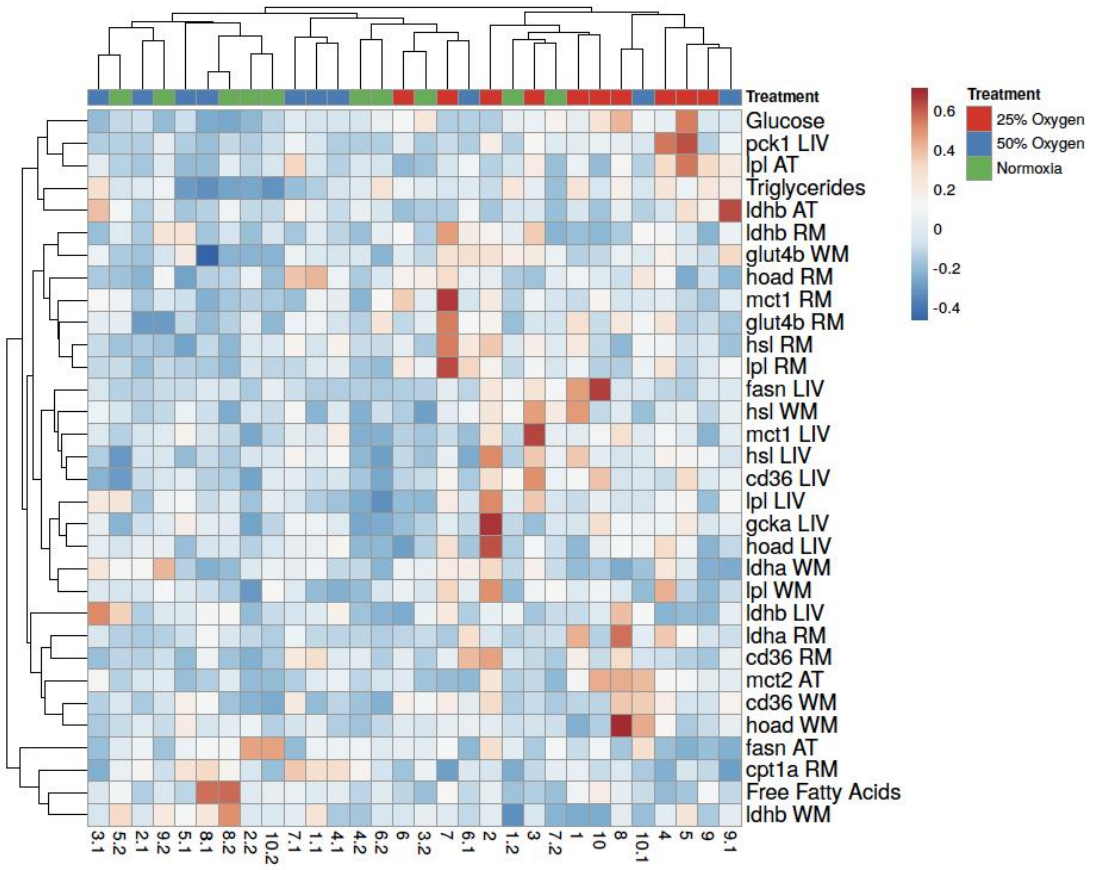

Figure 14. Heatmap in which both rows and columns are clustered using correlation distance and average linkage. Rows are centered, and vector scaling is applied to rows. Nipal's PCA is used for missing value estimation.

2.4. Discussion

2.4.1. Stable steady-state concentrations of circulating glucose and lipid oxidative fuels are maintained under acute hypoxia

We here show that an acute, 4 h exposure to gradually decreasing environmental hypoxia maintained at 50% and 25% of normoxia H_2O saturation for the final 2 h of the 4 h exposure does not affect the steady-state concentrations of circulating glucose, triglyceride and free fatty acids sampled at the end of the exposure, These findings are largely in line with the reported lack of, or moderate and transient nature of, concentration changes of these metabolites following acute hypoxia exposures of similar degree and duration in rainbow trout. For example, glucose concentrations did not differ between *a priori* collected terminally sampled normoxic fish blood samples and terminally collected blood samples after 3 h of acute hypoxia exposure following a rapid, 20 min reduction from normoxia to 20% O_2 saturation levels (Dunn & Hochachka, 1986). Similarly, a lack of statistically significant increase in glucose concentration change was also reported in rainbow trout exposed to ~20% O_2 saturation for 3 h, where blood was collected via dorsal cannulation (Dunn & Hochachka, 1987). Plasma glucose concentrations reached 6.3 mM under normoxia and 8.7 mM in 25% hypoxia. In contrast, other studies showed moderate and transient, yet significant increases in plasma glucose concentration in cannulated rainbow trout acutely challenged with a 25% hypoxia exposure period (Haman *et al.*, 1997). In this study, samples collected 30 and 60 min after stable environmental O_2 saturation levels of 25% were reached increased significantly from ~5 nM in normoxia to a steady state concentration of ~7mM under 25% O_2 saturation hypoxia after 30 and 60 min, before returning to slightly lower concentrations not significantly different from initial normoxia values after 90 min (Haman *et al.*, 1997). A mild, yet significant increase from 4.9 mM in normoxia to 6.1 mM in hypoxia in

circulating glucose concentration has been reported in rainbow trout exposed to 25% hypoxia for a period of 2.5 h following a gradual reduction from normoxia over a period of 1.5 h (Omlin & Weber, 2010). In triploid rainbow trout exposed to acute hypoxia in a more complex design that consisted of an initial period of sealing a 400 L group tank to lower O_2 from 7 mg/L O_2 (normoxia) to 5 mg/L via natural O_2 consumption followed by a rapid 10 min reduction to 2 mg/L over an additional 10 min to mimic 'aquaculture operation conditions' that induced mortality in some fish, sampled surviving fish exhibited significant increases in circulating glucose from 5.1 mM to 7.1 mM (Han *et al.*, 2022). Given the experimental design and significant mortality in parts of the exposure group, however, the comparability to other, sublethal experiments discussed previously is limited. Overall, the lack of significant changes in circulating glucose concentrations between trout exposed to normoxia and either level of acute hypoxia are similar to previously reported circulating glucose concentrations following acute hypoxia exposure in rainbow trout.

Similarly to glucose, no significant changes were detected in circulating triglyceride and free fatty acid concentrations, suggesting a tight regulation of steady-state concentrations of circulating lipid fuels under acute hypoxia exposure. Again, these findings are in line with a previously reported lack of changes (0.99 mM in normoxia compared to 0.12 mM in hypoxia) in the sum of measured NEFA in rainbow trout plasma following exposure to 25% O_2 saturation for a period of 90 min (Haman *et al.*, 1997). Of note, not only total concentrations, but also composition of plasma NEFAs did not change with acute hypoxia exposure (Haman *et al.*, 1997), suggesting the measurement of total free fatty acids is appropriate. In triploid rainbow trout exposed to acute hypoxia to mimic 'aquaculture operation conditions' that induced mortality in some fish, sampled surviving fish exhibited significant increases in circulating triglycerides from 4.3 mM to 5.3 mM (Han *et al.*, 2022). Again, these findings are in line with the identified lack of

change in circulating triglycerides and FFA between treatment groups in the current study.

Overall, these measurements of circulating metabolites support a tight regulation of glucose and lipid fuels, and thus a steady state of concentration which is robust to acute 4h hypoxia exposures at 50-25% O_2 saturation in rainbow trout. However, and importantly, the maintenance of these steady-state concentrations has been linked to changes in metabolite fluxes and metabolite turnover in previous studies using radioactive tracing in rainbow trout in similar experimental set-ups (Dunn & Hochachka, 1987; Haman *et al.*, 1997; Omlin & Weber, 2010). Briefly, metabolites can appear in circulation at specific rates (rate of appearance; R_a) or be disposed from circulation at specific rates (rate of disposal; R_d). In case of steady-state metabolite concentrations, R_a and R_d are, by definition, in equilibrium, but can concurrently increase or decrease depending on metabolite turnover (Weber *et al.*, 2016). Indeed, such changes have been measured for glucose, lactate and, free fatty acids in rainbow trout under experimental conditions of acute hypoxia exposure in which both degree and duration were comparable to our current study. For example, these studies identified a significant transient significant increase in glucose turnover at the onset, but not the end of acute hypoxia exposure (Haman *et al.*, 1997), concomitant increases in R_a and R_d lactate with $R_a > R_d$ (Omlin & Weber, 2010), as well as significant continuous decrease in FFA turnover (Haman *et al.*, 1997). Together, these findings suggest tissue-specific (molecular) mechanisms underlie coordinated and balanced changes in fluxes and turnover of plasma metabolites to maintain steady-state concentrations under chronic hypoxia.

2.4.2. Steady-state concentrations of circulating lactate and cortisol increase under short-term severe hypoxia

While the main oxidative fuels in rainbow trout (glucose, triglycerides, and free fatty acids) maintain stable steady-state concentrations under hypoxia exposure, the same cannot be said for

known hypoxia stress indicators. Plasma lactate levels were shown to increase non-significantly when exposed to 50% O_2 saturation and significantly when exposed to 25% O_2 saturation. Acute hypoxia exposure at 25% oxygen saturation was shown to increase steady state concentrations of circulating lactate from 0.6 mM under normoxia to 7 mM under 3 h of hypoxia (Dunn & Hochachka, 1986), and from 1 mM under normoxia to 8.9 mM under 1.5 h of hypoxia (Omlin & Weber, 2010) measured in rainbow trout blood collected after the exposures. Previous instances of increased blood lactate levels in rainbow trout have been shown to be a result of an increase in both lactate R_a and R_d, with lactate R_d increasing to a lesser extent (Omlin & Weber, 2010). While not measured in this study, lactate levels have also been shown to increase in multiple rainbow trout tissues under hypoxia exposure, including the heart, brain, liver, and red and white muscle, with white muscle as the major producer (Dunn & Hochachka, 1986; Omlin & Weber, 2010). An examination of changes in levels of lactate metabolism enzymes in different tissues under hypoxia could provide more details about lactate production in different tissues.

Similar to plasma lactate, this study also showed that plasma cortisol levels increase non-significantly when exposed to 50% O_2 saturation and significantly when exposed to 25% O_2 saturation. Cortisol is the main corticosteroid produced by the hypothalamo-pituitary-interrenal (HPI) axis in fish and is a reliable indicator of stress (Barcellos *et al.*, 2007; Sadoul & Geffroy, 2019). Exposure to severe hypoxia (4.2 kPa) for 5 hours (Williams *et al.*, 2019) and exposure to a rapid decrease in dissolved O_2 from 5 mg/L to 2 mg/L over 10 minutes (Han *et al.*, 2022) strongly increased cortisol levels in rainbow trout. The non-significant increase in cortisol under the exposure to 50% oxygen saturation could suggest that cortisol levels may being to increase under more moderate exposure to hypoxia, but more research on the response to the HPI axis under grades hypoxia exposure is required to confirm or refute this.

2.4.3. Tissue-specific transcript changes following acute hypoxia are indicative of metabolic plasticity

To assess tissue-specific molecular changes, we profiled the relative abundance of transcripts involved in key steps of glucose, lactate and lipid transport and metabolism in liver, red and white muscle, and visceral adipose tissue. While more immediate regulation of tissue metabolism is dependent on rapid regulation of protein conformation via post-translational modifications (PTMs) to regulate, for example, enzyme activity, transcriptional regulation of metabolic pathways nevertheless plays important roles in metabolic responses (Desvergne *et al.*, 2006) and has been shown to be regulated in rainbow trout in similarly acute time windows (Forbes *et al.*, 2019; Jubouri *et al.*, 2021; Mennigen *et al.*, 2012; Talarico *et al.*, 2023). Importantly, this allows us to probe the emerging regulatory roles of (O_2-sensitive) epigenetic marks including DNA methylation and histones in regulating metabolic gene transcription (Johnston *et al.*, 2025).

2.4.4. Hepatic transcript abundance of glucose/lactate and lipid metabolism-related gene expression are gradually induced depending on the degree of acute hypoxia exposure

We observed the highest number of transcript changes (n=6) and the lowest threshold of transcript level responses to acute hypoxia in hepatic tissue. This is in line with its reported highest degree of metabolic plasticity demonstrated by a significant reduction in amount of ATP, total adenylate content, creatine phosphate, and energy charge not found to the same extent in red and white muscle, heart muscle and brain in trout exposed to acute hypoxia (Dunn & Hochachka, 1986). Both the transcripts coding for one of two glucokinase paralogues (*gckb*), and the monocarboxylate transporter 1 (*mct1)*, were significantly induced at 50% O_2 saturation hypoxia exposure. GCK is a hepatic hexokinase isoform with a comparative Km which catalyzes the first step of glycolysis to phosphorylate imported glucose to retain in the cytoplasm but is not sensitive to its feedback.

MCT1 belongs to the family of monocarboxylate transporters and is dependent on the proton gradient, involved in lactate uptake (Omlin & Weber, 2010).

The rapid induction of *gckb* transcript at 50% O_2 saturation is in line with expected shifts toward anerobic ATP producing glycolysis. Indeed, acute hypoxia exposure of rainbow trout not only significantly decreased energy charge, but also significantly increased hepatic glucose-6-phosphate concentrations in rainbow trout exposed to acute hypoxia (Dunn & Hochachka, 1986). Thus, rapid induction of hepatic *gckb* at comparatively low thresholds of acute chronic hypoxia at least partially contributes to activation and/or maintenance of increased glycolytic responses in liver tissue to counter rapid loss in energy charges. Induction of *gckb*, but not *gcka,* was also observed in rainbow trout alevins following a previous exposure 24 h exposure to hypoxia (Liu *et al.*, 2017), suggesting that this molecular response is robust and occurs across different life-stages. The increase in hepatic glucokinase transcript in response to acute hypoxia is likely directly mediated at the level of the hepatic tissue, as a 1 h incubation of isolated primary trout and rat hepatocytes acutely increased *gck* transcript abundance (Rissanen *et al.*, 2006; Roth *et al.*, 2004). Thus, the lower threshold and rapid induction of *gckb* transcript in the liver supports the hypothesis of a preferred use of the glycolytic pathway in the liver, and an at least partial regulation at the transcript level. In line with this, consistent increases in activity of glycolytic enzymes have been reported in liver of rainbow trout exposed to hypoxia for 12 h (Wu *et al.*, 2024). Conversely, we did not identify an induction of the *ldha*, which codes for a lactate dehydrogenase A paralogue involved in the conversion of pyruvate to lactate in anerobic glycolysis. This response contrasts with described hypoxia-responsive induction of the *LDHA* isoform in mammals (Firth *et al.*, 1995) (Firth *et al.*, 1995) and suggests that transcriptional induction of hepatic *ldha* is not part of the immediate response required to induce glycolysis. In agreement with this finding, a lack of hepatic

ldha transcript induction was also observed in alevins exposed to 24 h hypoxia (Liu *et al.*, 2017), and adult rainbow exposed to acute hypoxia challenges (Han *et al.*, 2022). It is likely, however that LDH is acutely regulated at the activity level in the rainbow trout liver under acute hypoxia, as hepatic lactate concentrations increase significantly compared to normoxia after 3 h of hypoxia (Dunn & Hochachka, 1986) and hepatic LDH activity is increased after 12 h of liver hypoxia exposure. Interestingly, we also observed a low-threshold response for *mct1* induction, suggesting a response towards increased lactate import capacity which may indeed contribute to lactate clearance through the liver. Lactate was shown to increase in rainbow trout plasma in this study as well as previous lactate flux studies (Omlin & Weber, 2010). In line with this finding, a role for the liver in lactate clearance in rainbow trout has been demonstrated *in vivo* following hepatic ligation studies (Milligan & Girard, 1993). While this suggests a contribution of increased import capacity via *mct1* transcripts, the fate of imported lactate is less clear. Under normoxic resting conditions, the majority of imported lactate is oxidized (Milligan & Girard, 1993), but whether this is the case under more O_2 limiting conditions not established.

Somewhat surprisingly, we observed a strong increase in hepatic *pck1* expression, albeit only at the more severe hypoxia conditions tested. Similar to our finding, a robust increase in hepatic *pck1* abundance has recently been reported in adult rainbow trout following a more rapidly induced exposure to hypoxia (Han *et al.*, 2022), but not embryos or alevins. Whether this induction is linked to increased gluconeogenesis is unknown and the evidence for the functional metabolic relevance is mixed. While early studies suggested that *de-novo* synthesis of glucose under acutely hypoxic conditions from increased hepatic lactate or other precursors such as glycerol or amino acids is unlikely to occur in the trout liver given its sensitivity to reduced energy charge in acute hypoxia (Dunn & Hochachka, 1986), recent studies in the nematode *Caenorhabditis elegans*

demonstrated not only a robust induction of *pck1*, but also a role of its regulation of glucogenesis in hypoxia tolerance (Vora *et al.*, 2022). In our study, hepatic *pck1* abundance correlated strongly with circulating glucose measurements, and additional work probing the potential relevance of gluconeogenesis or futile hepatic glucose cycling in hypoxia trout hypoxia tolerance is warranted. With regard to the source of induction, it is unlikely to be mediated by lactate or its signalling directly, given that lactate infusion reduces both hepatic *pck1* transcript and Pck1 protein abundance over the same timeframe in normoxic trout (Talarico *et al.*, 2023). Conversely, *pck1* is strongly induced by the endocrine stress axis hormone cortisol, especially in fasted trout (Marandel *et al.*, 2019). The increase in plasma cortisol under the more severe hypoxia exposure shown in this study and previous studies (Han *et al.*, 2022) provides evidence that an increased stress response was responsible for the increase in hepatic *pck1* levels. In addition to *pck1*, the stronger acute hypoxia exposure also concurrently induced hepatic genes involved in fatty acid liberation (*lpl*), uptake (*cd36*), and synthesis (*fasn*) with highly correlated expression. Conversely, no significant changes in the *hoad* transcript were observed, which codes for a β-oxidation enzyme whose acute expression change has been previously linked to corresponding activity changes in rainbow trout (Talarico *et al.*, 2025). As such, the observed changes point to an increased capacity of fatty acid cycling in the liver, rather than use towards oxidative metabolism. In this context, the induction of *pck1* could arguably be linked to glyceroneogenesis, providing substrate for fatty acids to re-esterify into TAG. However, both glyceroneogenesis, as well as fatty acid synthesis are energetically costly and would directly oppose the benefits of a (lower hypoxia-threshold-dependent) activation of anaerobic glycolysis to balance (reduced) ATP generation with O_2 saving potential in the rainbow trout liver responsive at lower thresholds. Potential metabolic and non-metabolic explanations exist. First, as transcript abundance temporally precedes protein synthesis

and activity, such changes may be compensatory responses to changes in circulating FA turnover (Haman *et al.*, 1997) or preparatory changes for reoxygenation events in which FA oxidation and oxidative metabolism in general would quickly replenish diminished hepatic energy charges (Dunn & Hochachka, 1986). Secondly, while FA/TG re-esterification and turnover is high in rainbow trout, possibly to allow for rapid restructuring of phospholipids in this ectoderm (Magnoni *et al.*, 2008), it may be further increased in the liver under acute hypoxia to scavenge peroxidized lipids. In line with this possibility, an increase in malondialdehyde, an endogenous genotoxic product of enzymatic and oxygen radical-induced lipid peroxidation has been quantified in rainbow trout plasma and to a lesser extent liver in rainbow trout following acute hypoxia exposure. Indeed, hypoxia-induced induction of *cd36* has been previously reported and was hypothesized to be linked to scavenging of lipid peroxidation products. If this hypothesis is true, then our exposure range and molecular data delineate specific acute hypoxia exposure thresholds for activation of metabolically beneficial, and O_2 conserving metabolic pathways such as glycolysis (as low as 50% O_2 saturation) and the metabolically costly, but oxidative stress protective induction of lipid turnover pathways at 25% O_2 saturation. Interestingly, acute induction of *CD36* mRNA and CD36 protein under severe, 6 h hypoxia exposure has been described in different human tissue cell lines *in vitro* (Mwaikambo *et al.*, 2009). This upregulation was not only dependent on reactive oxygen species (ROS), but also functionally linked to increased uptake of oxidized low density lipoprotein components (Mwaikambo *et al.*, 2009). Future studies should therefore investigate the role of antioxidants on markers of lipid peroxidation, the induction of lipid metabolism-related gene expression, and energy charge in the hypoxic rainbow trout liver to formally test this hypothesis. In line with non-energy metabolism-related roles of components of hepatic lipid metabolism, *fasn*, reported to be induced along with other lipid metabolism related genes under hypoxia in cancer

cells (Mylonis *et al.*, 2019), has also been linked to stabilize HIF-1α via direct interaction with the von Hippel-Lindau tumour suppressor protein (pVHL) to replace the E3 ubiquitin ligase complex (Sun *et al.*, 2017).

2.4.5. White and red muscle tissue transcripts involved in glucose and lipid metabolism are differentially regulated under acute hypoxia exposure

Compared to liver tissue, fewer changes in transcripts relevant to energy metabolism were differentially expressed in acute hypoxia, and all significant changes compared to normoxia occurred at the highest degree of hypoxia tested (25% saturation). This is in line with fewer effects on energy reserves in red and white muscle under chronic hypoxia compared to liver (Dunn & Hochachka, 1986). Nevertheless, and in line with increased glucose use, a significant increase in *glut4b* abundance was found in white but not red muscle of hypoxia-exposed rainbow trout. This mimics transcriptional responses observed followed lactate infusion in normoxic trout, suggesting that this induction may be lactate dependent. In support of a need for increased capacity for glucose import in white muscle under acute hypoxia, a recent study identified significant activity increases in the glycolytic enzymes' hexokinase in this tissue (Wang *et al.*, 2025). In rainbow trout exposed to acute hypoxia or intense exercise, white muscle is a significant source of lactate, which is, however, mostly fueled from endogenous glycogen (Dunn & Hochachka, 1986, 1987; Milligan & Girard, 1993; Omlin & Weber, 2010). In contrast to the mammalian Cori-cycle, lactate is then largely used *in situ* to replenish glycogen reserves. Similar to liver tissue, no changes in *ldh* transcripts (*a* or *b*) is found in the either muscle tissue, suggesting that regulation is not dependent on transcriptionally mediated increases LDH abundance, but rather protein level regulation. In line with this finding, lactate concentrations were found to increase drastically and rapidly in response to 3 h acute hypoxia (Dunn & Hochachka, 1986), while increased LDH activity was measured in

whole trout muscle following 4 h hypoxia exposure (Wang *et al.*, 2025). Regarding lipid metabolism-related transcripts, induction of *lpl* transcripts in red muscle and *cd36* in white muscle suggest, especially in light of high degree of correlation in expression between tissues in individuals, a coordinated response of induction across multiple tissues in rainbow trout exposed to higher degrees of acute hypoxia exposure. In agreement with previously discussed limitations considering aerobic use of FA to generate energy, it is uncertain whether these changes in red muscle are linked to increased FA import for oxidation, especially given a lack of change in *cpt1a* abundance in this tissue (data not shown).

In adipose tissue, the induction of *mct2* suggests, similarly to liver tissue, a metabolic response to increase lactate uptake under hypoxia. Interestingly, and in contrast to mammals, where lactate signalling in adipose tissue is linked to reductions in adipocyte lipolysis, this response does not appear to occur in rainbow trout (Talarico *et al.*, 2025). Similarly to other tissues no induction of *ldha* was observed in adipose tissue following acute hypoxia exposure. Therefore, the observed induction in *lpl* is in line with this previous finding and suggest a transcriptionally mediated increase to enhance tissue capacity for fatty acid mobilization.

2.4.6. The differential induction of hepatic transcripts mct1 and pck1 in response to acute hypoxia is not strongly linked to changes in H3K4me3 marks upstream of TSS

We did not identify global changes in DNA 5C-methylation levels in hepatic tissue. Global DNA methylation level changes have been demonstrated to occur in response to very severe hypoxia exposures of <1% saturation in cancer cells *in vitro*, where they have been shown to be linked to decreased TET demethylase activity that is directly dependent on O_2. Under the current acute hypoxia exposure regime, such near anoxic tissue concentrations are not reached. However, it remains feasible that individual CpG islands are differentially methylated to regulate

transcription, but these changes are likely not direct or globally dependent on O_2 under our experimental design.

In contrast to DNA methylation, specific histone marks, including H3K4me3, a mark associated with active gene expression, H3K27me3, a mark associated with silent genes, and H3K36me3, bivalent poised mark, have been shown to be directly dependent on cellular O_2 concentrations closer to the physiological range of less strong O_2 affinity of the known PhD/Egln sensors regulating HIF-1α stability (Johnston *et al.*, 2025). Given that transcripts profiled in liver tissue were most responsive to acute hypoxia exposure and exhibited transcripts with graded responses with inductions at both (*mct1*) or only more severe hypoxia exposure (*pck1*), we investigated whether changes in O_2-sensitive histone marks upstream of TSS underlie changes in transcript abundance. Because these transcripts were induced, we hypothesized that hypoxia would specifically act to stabilize H3K4me3 marks at these loci, and especially the region surrounding the TSS. Contrary to our predictions, while changes in H3K4me3 marks were observed for the *pck1*, but not mct1 sites upstream of TSS, we found a significant decrease in H3K4me3/H3 ratios in the regions furthest upstream of the TSS, suggesting decreased writing and/or increased erasure of these marks. Conversely, marks closer to the TSS did not reveal significant changes in H3K4me3/H3 ratios. When investigating correlations between *pck1* transcript abundance and specific upstream region H3K4me3/H3 ratios in individuals across all treatment groups, no significant correlations were identified, except for a positive and significant correlation in region close to the TSS. As the trout liver is a homogenous tissue, it is assumed that separate fractions of the same individual sample used to extract RNA for cDNA synthesis and subsequent *real-time* RT PCR on the one hand and DNA extractions for chromatin shearing and ChIP assays on the other are suitable for correlational analyses between transcript abundance and histone marks. Neither

changes in H3K4me3/H3 ratio in regions upstream of the *mct1* gene nor significant positive correlations between upstream H3K4me3/H3 ratio and *mct1* transcript abundance were identified. Together, these changes suggest that hypoxia-dependent H3K4me3/H3 regulation upstream of induced hepatic genes plays a small, if any role in mediating induction of these transcripts.

While not investigated in this thesis, transcript abundance depends, in addition to its synthesis, also on its half-life and degradation. In addition to transcriptionally active epigenetic mechanisms (DNA methylation, histone modifications), posttranscriptional mechanisms, especially miRNAs, may act to degrade mRNA transcripts and/or inhibit their translation (Mennigen, 2016). Future studies using combinations of *in silico* 3'UTR target prediction algorithms in conjunction with targeted miRNA expression analysis may be used to explore this possibility (Kostyniuk & Mennigen, 2020).

The acute induction of metabolism-related transcripts under acute hypoxia may be furthermore dependent on several other transcriptional mechanisms. Several of the transcripts found to be induced by reported to be induced by hypoxia in mammalian cells *in vitro*, have been reported to be HIF-1α target genes in other species. In absence of suitable HIF-1α antibodies in fishes, the activation and direct regulation of gene-specific transcription for this pathway, remains challenging. Surprisingly, and despite the confirmation of decreases and maintenance of environmental O_2 concentrations at target levels (normoxia, 50% O_2 saturation, 25% O_2 saturation), we did not observe induction of *egln3* at the level of the gene in any tissue under either hypoxic condition. It is unlikely that this discrepancy is linked to the investigation of only one of two paralogues, as both exhibited robust, concurrent induction rainbow trout embryos exposed to hypoxia. However, our hypoxia exposure duration of 4 h was more acute compared to previous studies, which tended to be more chronic in nature. As such, it is possible that *egln3* transcript

induction requires longer than acute timeframes, rendering limiting its utility as robust molecular marker of HIF-1α signaling in more acute hypoxia exposures. The fact that it represents a feedback loop with the HIF-1α pathway may mean an initial suppression as HIF-1α is induced, although this would require further examination.

Outside of direct O_2-sensitive molecular (HIF-1α) or epigenetic regulation of transcripts, other factors may contribute to the observed changes in transcript abundance. Components of both the neuronal (catecholamines) and endocrine (cortisol) stress response are of particular interest, given their reported rapid increase in response to acute hypoxia-exposure in rainbow trout (Han *et al.*, 2022; Perry, 1998). Catecholamines are among the only compounds tested in rainbow trout that are capable of modulating lipolytic rates assessed as by plasma glycerol (Weber *et al.*, 2016). Cortisol is known to increase under severe hypoxic conditions (Han *et al.*, 2022) and is a potent regulator of *pck1* transcription via the glucocorticoid receptor GR in trout acting, as in other species (Marandel *et al.*, 2019), on GRE elements. Indeed, several putative GRE elements were identified in the upstream region of *pck1* using an *in-silico* screen (data not shown). Future pharmacological cortisol manipulation experiments and ChIP assays using available trout GR-specific antibodies (Sathiyaa & Vijayan, 2003) would be necessary to resolve this question.

3. General conclusions

In this thesis, I investigated metabolic responses to different levels of hypoxia at the circulating steady-state-metabolite level, and tissue-specific molecular level. The steady-state concentration of key fuel metabolites (glucose, triglycerides, free fatty acids) is unaltered under chronic hypoxia, suggesting a tight regulation, while known hypoxia stress markers (lactate and

cortisol) increased under severe hypoxia exposure. In line with previously established changers in fluxes in the same set-up, investigation of key transcripts with roles in glucose, lactate and lipid metabolism reveal rapid tissue specific changes, suggesting the rapid metabolic responses involve transcriptional and/or possible mRNA degradation changes and modulate tissue-specific fluxes of metabolic fuels. We observed the most sensitive and comprehensive transcriptional changes in hepatic tissue, in line with the previously reported most dramatic decreases in energy charge in this tissue in rainbow trout exposed to acute hypoxia. The most sensitive transcript changes in liver tissue occur for glycolytic metabolism-related genes at 50% O_2 saturation, in line with the hypothesis that transcriptional changes contribute to a prioritization of anerobic metabolic pathways. This is further supported by O_2 saturation-dependent increases in glucose 4 transporters in white muscle, suggesting an enhanced need for and metabolic reliance on glucose uptake into this tissue. However, both lactate dehydrogenase isoforms examined showed no induction under either the mild or severe hypoxia responses, suggesting that lactate metabolism is a longer-term response to hypoxia. The liver was the most oxygen-dependent tissue examined, and the examination of other oxygen-dependent tissues like the heart and the brain may reveal an earlier induction of lactate metabolism.

Unexpectedly, several components involved in lipid metabolism showed concerted induction within liver tissue and between tissues, however this was only following exposure to 25% O_2 saturation. While transcript markers of oxidative use, especially enzymes involved in β-oxidation do not change and thus support a lack of aerobic fuel use, we propose that the induction of components of free fatty acid liberation, uptake and re-synthesis in the liver may contribute to an adaptive response to lipid peroxidation, a hypothesis that warrants further testing.

Following the development of a theoretical framework in form a review paper (Johnston *et al.*, 2025), I also investigated the potential contribution of O_2-sensitive epigenetic machinery to observed induction of transcripts in the liver. While global DNA methylation level did not change in hepatic tissue under our acute hypoxia exposure, conditions, in line with expected lower hypoxia-thresholds for DNA demethylation enzymes described *in vitro*, we observed significant changes in the O_2-sensitive and permissive epigenetic mark HK4me3 in promotor regions of *pck1*, but not *mct1*. However, contrary to my predictions, H3K4me3 levels were not stabilized or increased in response to O_2 in the putative promotor regions of both genes, suggesting alternative mechanisms are involved in transcriptional activation. In spite of a lack of the *bona fide* transcriptional marker of *egln3*, at least some of the induced target genes have been shown be directly regulated by HIF-1α. However, in absence of reliable antibodies, direct investigation of HIF-1α binding via ChIP assays remains a challenge. Conversely, the observed induction of transcripts at lower O_2 saturation levels warrants future investigation of cortisol levels, especially since a validated antibody for GR exists in rainbow trout that could be tried in ChIP assays. Finally, while representing a first step, the successful use of a ChIP assay developed in this thesis opens the avenue for comparative investigation of the role of the role of O_2- sensitive epigenetic regulation of transcription under hypoxia in more tolerant species, such as goldfish or zebrafish. The latter provides the intriguing possibility to use HIF-1α knock-outs to dissociate epigenetic from HIF-dependent O_2-sensing-mediated regulation of metabolic and/or other pathways contributing to hypoxia tolerance in this species.

4. References

Altringham, J. D., & Ellerby, D. J. (1999). Fish swimming: patterns in muscle function. *Journal of Experimental Biology*, *202*, 3397–3403.

Barcellos, L. J. G., Ritter, F., Kreutz, L. C., Quevedo, R. M., da Silva, L. B., Bedin, A. C., … Cericato, L. (2007). Whole-body cortisol increases after direct and visual contact with a predator in zebrafish, *Danio rerio*. *Aquaculture*, *272*, 774–778.

Batie, M., Frost, J., Frost, M., Wilson, J. W., Schofield, P., & Rocha, S. (2019). Hypoxia induces rapid changes to histone methylation and reprograms chromatin. *Science*, *363*, 1222–1226.

Bickler, P. E., & Buck, L. T. (2007). Hypoxia Tolerance in Reptiles, Amphibians, and Fishes: Life with Variable Oxygen Availability. *Annual Review of Physiology*, *69*, 145–170.

Binda, O., LeRoy, G., Bua, D. J., Garcia, B. A., Gozani, O., & Richard, S. (2010). Trimethylation of histone H3 lysine 4 impairs methylation of histone H3 lysine 9. *Epigenetics*, *5*, 767–775.

Braz-Mota, S., & Almeida-Val, V. M. F. (2021). Ecological adaptations of Amazonian fishes acquired during evolution under environmental variations in dissolved oxygen: A review of responses to hypoxia in fishes, featuring the hypoxia-tolerant Astronotus spp. *Journal of Experimental Zoology Part A: Ecological and Integrative Physiology*, *335*, 771–786.

Burggren, W. W. (1982). 'Air Gulping' Improves Blood Oxygen Transport during Aquatic Hypoxia in the Goldfish Carassius auratus. *Physiological Zoology*, *55*, 327–334.

Bushnell, P. G., & Brill, R. W. (1992). Oxygen transport and cardiovascular responses in skipjack tuna (Katsuwonus pelamis) and yellowfin tuna (Thunnus albacares) exposed to acute hypoxia. *Journal of Comparative Physiology B*, *162*, 131–143.

Carter, A. M., Blaszczak, J. R., Heffernan, J. B., & Bernhardt, E. S. (2021). Hypoxia dynamics and spatial distribution in a low gradient river. *Limnology and Oceanography*, *66*, 2251–2265.

Cerra, M. C., Filice, M., Caferro, A., Mazza, R., Gattuso, A., & Imbrogno, S. (2023). Cardiac Hypoxia Tolerance in Fish: From Functional Responses to Cell Signals. *International Journal of Molecular Sciences*, *24*, 1460.

Cortes, S., Farhat, E., Talarico, G., & Mennigen, J. A. (2024). The dynamic transcriptomic response of the goldfish brain under chronic hypoxia. *Comparative Biochemistry and Physiology Part D: Genomics and Proteomics*, *50*, 101233.

Craig, P. M., Fitzpatrick, J. L., Walsh, P. J., Wood, C. M., & McClelland, G. B. (2014). Coping with aquatic hypoxia: how the plainfin midshipman (Porichthys notatus) tolerates the intertidal zone. *Environmental Biology of Fishes*, *97*, 163–172.

Davis, J. C. (1975). Minimal Dissolved Oxygen Requirements of Aquatic Life with Emphasis on Canadian Species: a Review. *Journal of the Fisheries Board of Canada*, *32*, 2295–2332.

Desvergne, B., Michalik, L., & Wahli, W. (2006). Transcriptional regulation of metabolism. *Physiological Reviews*, *86*, 465–514.

Diaz, R. J., & Rosenberg, R. (2008). Spreading Dead Zones and Consequences for Marine Ecosystems. *Science*, *321*, 926–929.

Domenici, P., Herbert, N. A., Lefrançois, C., Steffensen, J. F., & McKenzie, D. J. (2013). The Effect of Hypoxia on Fish Swimming Performance and Behaviour. In A. P. Palstra & J. V. Planas (Eds.), *Swimming Physiology of Fish: Towards Using Exercise to Farm a Fit Fish in Sustainable Aquaculture* (pp. 129–159). Berlin, Heidelberg: Springer.

Dunn, J. F., & Hochachka, P. W. (1986). Metabolic Responses of Trout (*Salmo Gairdneri*) To Acute Environmental Hypoxia. *Journal of Experimental Biology*, *123*, 229–242.
Dunn, J. F., & Hochachka, P. W. (1987). Turnover rates of glucose and lactate in rainbow trout during acute hypoxia. *Canadian Journal of Zoology*, *65*, 1144–1148.
Eames, S. C., Philipson, L. H., Prince, V. E., & Kinkel, M. D. (2010). Blood sugar measurement in zebrafish reveals dynamics of glucose homeostasis. *Zebrafish*, *7*, 205–214.
Firth, J. D., Ebert, B. L., & Ratcliffe, P. J. (1995). Hypoxic Regulation of Lactate Dehydrogenase A: INTERACTION BETWEEN HYPOXIA-INDUCIBLE FACTOR 1 AND cAMP RESPONSE ELEMENTS (∗). *Journal of Biological Chemistry*, *270*, 21021–21027.
Forbes, J. L. I., Kostyniuk, D. J., Mennigen, J. A., & Weber, J.-M. (2019). Glucagon regulation of carbohydrate metabolism in rainbow trout: in vivo glucose fluxes and gene expression. *Journal of Experimental Biology*, *222*, jeb211730.
García-Meilán, I., Tort, L., & Khansari, A. R. (2022). Rainbow trout integrated response after recovery from short-term acute hypoxia. *Frontiers in Physiology*, *13*.
Gatz, A. J. (1973). Speed, Stamina, and Muscles in Fishes. *Journal of the Fisheries Board of Canada*, *30*, 325–328.
Gerber, L., Resseguier, J., Helle-Valle, T., Farhat, E., Nilsson, G. E., & Lefevre, S. (2024). Expression of prolyl hydroxylase domains, the upstream regulators of HIF, in the brain of the anoxia-tolerant crucian carp during anoxia-reoxygenation. *American Journal of Physiology-Regulatory, Integrative and Comparative Physiology*, *326*, R184–R195.
Greenald, D., Jeyakani, J., Pelster, B., Sealy, I., Mathavan, S., & van Eeden, F. J. (2015). Genome-wide mapping of Hif-1α binding sites in zebrafish. *BMC Genomics*, *16*, 923.
Haman, F., Zwingelstein, G., & Weber, J.-M. (1997). Effects of hypoxia and low temperature on substrate fluxes in fish: plasma metabolite concentrations are misleading. *American Journal of Physiology-Regulatory, Integrative and Comparative Physiology*, *273*, R2046–R2054.
Han, B., Meng, Y., Tian, H., Li, C., Li, Y., Gongbao, C., … Ma, R. (2022). Effects of Acute Hypoxic Stress on Physiological and Hepatic Metabolic Responses of Triploid Rainbow Trout (*Oncorhynchus mykiss*). *Frontiers in Physiology*, *13*.
Henson, S. A., Beaulieu, C., Ilyina, T., John, J. G., Long, M., Séférian, R., … Sarmiento, J. L. (2017). Rapid emergence of climate change in environmental drivers of marine ecosystems. *Nature Communications*, *8*, 14682.
Iftikar, F. I., Matey, V., & Wood, C. M. (2010). The Ionoregulatory Responses to Hypoxia in the Freshwater Rainbow Trout *Oncorhynchus mykiss*. *Physiological and Biochemical Zoology*, *83*, 343–355.
Jane, S. F., Mincer, J. L., Lau, M. P., Lewis, A. S. L., Stetler, J. T., & Rose, K. C. (2023). Longer duration of seasonal stratification contributes to widespread increases in lake hypoxia and anoxia. *Global Change Biology*, *29*, 1009–1023.
Jenny, J.-P., Francus, P., Normandeau, A., Lapointe, F., Perga, M.-E., Ojala, A., … Zolitschka, B. (2016). Global spread of hypoxia in freshwater ecosystems during the last three centuries is caused by rising local human pressure. *Global Change Biology*, *22*, 1481–1489.
Johnston, W., Adil, S., Cao, C., Nipu, N., & Mennigen, J. A. (2025). Fish models to explore epigenetic determinants of hypoxia-tolerance. *Comparative Biochemistry and Physiology Part A: Molecular & Integrative Physiology*, *302*, 111811.

Jordan, A. D., Herbert, N. A., & Steffensen, J. F. (2005). Escape performance in three teleosts from West Greenland. *Polar Biology*, *28*, 164–167.

Jubouri, M., Talarico, G. G. M., Weber, J.-M., & Mennigen, J. A. (2021). Alanine alters the carbohydrate metabolism of rainbow trout: glucose flux and cell signaling. *Journal of Experimental Biology*, *224*, jeb232918.

Kostyniuk, D. J., & Mennigen, J. A. (2020). Meta-analysis of differentially-regulated hepatic microRNAs identifies candidate post-transcriptional regulation networks of intermediary metabolism in rainbow trout. *Comparative Biochemistry and Physiology Part D: Genomics and Proteomics*, *36*, 100750.

Li, L., Shen, S., Bickler, P., Jacobson, M. P., Wu, L. F., & Altschuler, S. J. (2023). Searching for molecular hypoxia sensors among oxygen-dependent enzymes. *eLife*, *12*, e87705.

Liu, J., Plagnes-Juan, E., Geurden, I., Panserat, S., & Marandel, L. (2017). Exposure to an acute hypoxic stimulus during early life affects the expression of glucose metabolism-related genes at first-feeding in trout. *Scientific Reports*, *7*, 363.

Ma, F., Zou, Y., Chen, X., Ma, L., & Ma, R. (2023). Evolution, characterization, and expression profile of Egl-9 family hypoxia-inducible factor (egln) in rainbow trout (Oncorhynchus mykiss) under hypoxia stress. *Animal Biotechnology*, *34*, 1753–1762.

MacCormack, T. J., & Driedzic, W. R. (2004). Cardiorespiratory and tissue adenosine responses to hypoxia and reoxygenation in the short-horned sculpin Myoxocephalus scorpius. *Journal of Experimental Biology*, *207*, 4157–4164.

Magnoni, L. J., Crespo, D., Ibarz, A., Blasco, J., Fernández-Borràs, J., & Planas, J. V. (2013). Effects of sustained swimming on the red and white muscle transcriptome of rainbow trout (*Oncorhynchus mykiss*) fed a carbohydrate-rich diet. *Comparative Biochemistry and Physiology Part A: Molecular & Integrative Physiology*, *166*, 510–521.

Magnoni, L., Vaillancourt, E., & Weber, J.-M. (2008). High resting triacylglycerol turnover of rainbow trout exceeds the energy requirements of endurance swimming. *American Journal of Physiology-Regulatory, Integrative and Comparative Physiology*, *295*, R309–R315.

Mandic, M., Best, C., & Perry, S. F. (2020). Loss of hypoxia-inducible factor 1α affects hypoxia tolerance in larval and adult zebrafish (Danio rerio). *Proceedings of the Royal Society B*, *287*, 20200798.

Mandic, M., Joyce, W., & Perry, S. F. (2021). The evolutionary and physiological significance of the Hif pathway in teleost fishes. *Journal of Experimental Biology*, *224*, jeb231936.

Marandel, L., Kostyniuk, D. J., Best, C., Forbes, J. L. I., Liu, J., Panserat, S., & Mennigen, J. A. (2019). Pck-ing up steam: Widening the salmonid gluconeogenic gene duplication trail. *Gene*, *698*, 129–140.

Mennigen, J. A. (2016). Micromanaging metabolism—a role for miRNAs in teleost energy metabolism. *Comparative Biochemistry and Physiology Part B: Biochemistry and Molecular Biology*, *199*, 115–125.

Mennigen, J. A., Panserat, S., Larquier, M., Plagnes-Juan, E., Medale, F., Seiliez, I., & Skiba-Cassy, S. (2012). Postprandial Regulation of Hepatic MicroRNAs Predicted to Target the Insulin Pathway in Rainbow Trout. *PLOS ONE*, *7*, e38604.

Milligan, C. L., & Girard, S. S. (1993). Lactate Metabolism In Rainbow Trout. *Journal of Experimental Biology*, *180*, 175–193.

Mwaikambo, B. R., Yang, C., Chemtob, S., & Hardy, P. (2009). Hypoxia Up-regulates CD36 Expression and Function via Hypoxia-inducible Factor-1- and Phosphatidylinositol 3-Kinase-dependent Mechanisms. *The Journal of Biological Chemistry*, *284*, 26695–26707.
Mylonis, I., Simos, G., & Paraskeva, E. (2019). Hypoxia-Inducible Factors and the Regulation of Lipid Metabolism. *Cells*, *8*, 214.
Naqvi, S. W. A., Bange, H. W., Farías, L., Monteiro, P. M. S., Scranton, M. I., & Zhang, J. (2010). Marine hypoxia/anoxia as a source of CH_4 and N_2O. *Biogeosciences*, *7*, 2159–2190.
Nilsson, G. E. (2001). Surviving Anoxia With the Brain Turned On. *Physiology*, *16*, 217–221.
Omlin, T., & Weber, J.-M. (2010). Hypoxia stimulates lactate disposal in rainbow trout. *Journal of Experimental Biology*, *213*, 3802–3809.
Omlin, T., & Weber, J.-M. (2013). Exhausting exercise and tissue-specific expression of monocarboxylate transporters in rainbow trout. *American Journal of Physiology-Regulatory, Integrative and Comparative Physiology*, *304*, R1036–R1043.
Omlin, T., Langevin, K., & Weber, J.-M. (2014). Exogenous lactate supply affects lactate kinetics of rainbow trout, not swimming performance. *American Journal of Physiology-Regulatory, Integrative and Comparative Physiology*, *307*, R1018–R1024.
Perry, S. F. (1998). Relationships Between Branchial Chloride Cells and Gas Transfer in Freshwater Fish. *Comparative Biochemistry and Physiology Part A: Molecular & Integrative Physiology*, *119*, 9–16.
Perry, S. F., Jonz, M. G., & Gilmour, K. M. (2009). Chapter 5 Oxygen Sensing And The Hypoxic Ventilatory Response. In J. G. Richards, A. P. Farrell, & C. J. Brauner (Eds.), *Fish Physiology* (pp. 193–253). Academic PressHypoxia.
Perry, S. F., Pan, Y. K., & Gilmour, K. M. (2023). Insights into the control and consequences of breathing adjustments in fishes-from larvae to adults. *Frontiers in Physiology*, *14*.
Pörtner, H. O., & Knust, R. (2007). Climate Change Affects Marine Fishes Through the Oxygen Limitation of Thermal Tolerance. *Science*, *315*, 95–97.
Rao, R. C., & Dou, Y. (2015). Hijacked in cancer: the KMT2 (MLL) family of methyltransferases. *Nature Reviews Cancer*, *15*, 334–347.
Rissanen, E., Tranberg, H. K., & Nikinmaa, M. (2006). Oxygen availability regulates metabolism and gene expression in trout hepatocyte cultures. *American Journal of Physiology-Regulatory, Integrative and Comparative Physiology*, *291*, R1507–R1515.
Rogers, N. J., Urbina, M. A., Reardon, E. E., McKenzie, D. J., & Wilson, R. W. (2016). A new analysis of hypoxia tolerance in fishes using a database of critical oxygen level (P_{crit}). *Conservation Physiology*, 1–20.
Roth, U., Jungermann, K., & Kietzmann, T. (2004). Modulation of glucokinase expression by hypoxia-inducible factor 1 and upstream stimulatory factor 2 in primary rat hepatocytes. *385*, 239–247.
Sadoul, B., & Geffroy, B. (2019). Measuring cortisol, the major stress hormone in fishes. *Journal of Fish Biology*, *94*, 540–555.
Sathiyaa, R., & Vijayan, M. M. (2003). Autoregulation of glucocorticoid receptor by cortisol in rainbow trout hepatocytes. *American Journal of Physiology-Cell Physiology*, *284*, C1508–C1515.
Strowbridge, N., Northrup, S. L., Earhart, M. L., Blanchard, T. S., & Schulte, P. M. (2021). Acute measures of upper thermal and hypoxia tolerance are not reliable predictors of

mortality following environmental challenges in rainbow trout (*Oncorhynchus mykiss*). *Conservation Physiology*, *9*, 1dk–1dk.
Sun, W., Kato, H., Kitajima, S., Lee, K. L., Gradin, K., Okamoto, T., & Poellinger, L. (2017). Interaction between von Hippel-Lindau Protein and Fatty Acid Synthase Modulates Hypoxia Target Gene Expression. *Scientific Reports*, *7*, 7190.
Svendsen, J. C., Steffensen, J. F., Aarestrup, K., Frisk, M., Etzerodt, A., & Jyde, M. (2012). Excess posthypoxic oxygen consumption in rainbow trout (*Oncorhynchus mykiss*): recovery in normoxia and hypoxia. *Canadian Journal of Zoology*, *90*, 1–12.
Talarico, G. G. M., Thoral, E., Farhat, E., Teulier, L., Mennigen, J. A., & Weber, J.-M. (2023). Lactate signaling and fuel selection in rainbow trout: mobilization of energy reserves. *American Journal of Physiology-Regulatory, Integrative and Comparative Physiology*, *325*, R556–R567.
Talarico, G. G. M., Farhat, E., Mennigen, J. A., & Weber, J.-M. (2025). Metabolic fuel selection in rainbow trout: coping with intralipid infusion. *American Journal of Physiology-Regulatory, Integrative and Comparative Physiology*, *328*, R306–R318.
Tellier, J. M., Kalejs, N. I., Leonhardt, B. S., Cannon, D., Höök, T. O., & Collingsworth, P. D. (2022). Widespread prevalence of hypoxia and the classification of hypoxic conditions in the Laurentian Great Lakes. *Journal of Great Lakes Research*, *48*, 13–23.
Teulier, L., Omlin, T., & Weber, J.-M. (2013). Lactate kinetics of rainbow trout during graded exercise: do catheters affect the cost of transport? *Journal of Experimental Biology*, *216*, 4549–4556.
Thienpont, B., Steinbacher, J., Zhao, H., D'Anna, F., Kuchnio, A., Ploumakis, A., … Lambrechts, D. (2016). Tumour hypoxia causes DNA hypermethylation by reducing TET activity. *Nature*, *537*, 63–68.
Vaage, B. M., Liss, S. A., Fischer, E. S., Khan, F., & Hughes, J. S. (2023). Can portable glucose and lactate meters be a useful tool in quantifying stress of juvenile Chinook salmon? *Conservation Physiology*, *11*, coad046.
Vora, M., Pyonteck, S. M., Popovitchenko, T., Matlack, T. L., Prashar, A., Kane, N. S., … Rongo, C. (2022). The hypoxia response pathway promotes PEP carboxykinase and gluconeogenesis in C. elegans. *Nature Communications*, *13*, 1–15.
Vornanen, M., Stecyk, J. A. W., & Nilsson, G. E. (2009). Chapter 9 The Anoxia-Tolerant Crucian Carp (*Carassius Carassius* L.). In J. G. Richards, A. P. Farrell, & C. J. Brauner (Eds.), *Fish Physiology* (pp. 397–441). Academic PressHypoxia.
Wang, L., Wang, J., Liu, Y., Liu, F., Lou, B., Chen, Y., & Zhu, J. (2025). Metabolic responses of small yellow croaker (*Larimichthys polyactis*) liver to hypoxic stress: Insights into glucose and lipid metabolism. *Aquaculture*, *598*, 742015.
Weber, J.-M. (2011). Metabolic fuels: regulating fluxes to select mix. *Journal of Experimental Biology*, *214*, 286–294.
Weber, J.-M., Choi, K., Gonzalez, A., & Omlin, T. (2016). Metabolic fuel kinetics in fish: swimming, hypoxia and muscle membranes. *Journal of Experimental Biology*, *219*, 250–258.
Williams, K. J., Cassidy, A. A., Verhille, C. E., Lamarre, S. G., & MacCormack, T. J. (2019). Diel cycling hypoxia enhances hypoxia tolerance in rainbow trout (*Oncorhynchus mykiss*): evidence of physiological and metabolic plasticity. *Journal of Experimental Biology*, *222*, jeb206045.

Wu, S., Huang, J., Li, Y., & Zhao, L. (2024). Comparative transcriptomics combined with physiological and functional analysis reveals the regulatory mechanism of rainbow trout (*Oncorhynchus mykiss*) under acute hypoxia stress. *Ecotoxicology and Environmental Safety*, *278*, 116347.